

**FATIGUE AND DAMAGE TOLERANCE ANALYSIS  
OF COMPOSITE LAMINATES —  
STIFFNESS LOSS, DAMAGE MODELLING,  
AND LIFE PREDICTION**

**BANGYAN LIU**

**A thesis submitted to the  
Faculty of Graduate Studies and Research  
in partial fulfillment of the requirement for  
the Degree of Master of Engineering**

**Department of Mechanical Engineering  
McGill University  
Montreal, Quebec, Canada H3A 2K6**

**© B. Y. LIU, MAY, 1992**

---

**ABSTRACT**

The prediction of fatigue life and evaluation of onset and growth of matrix cracks and delamination for general composite laminates are studied analytically using theories of damage tolerance, residual modulus degradation and residual strength degradation. Damage onset including matrix cracks and edge delamination are predicted by using a total strain energy release rate criterion which accounts for interactive effects of matrix cracks and delamination. Based on the assumption of a linear relation between damage and stiffness loss, the analytical models for modulus degradation, matrix crack density and delamination size growth as function of fatigue stress and fatigue cycles are proposed. The proposed approach provides four choices for predicting tension-tension fatigue life and for assessing fail-safety for structures made of composite laminates: residual modulus criterion, matrix cracking criterion, delamination size criterion and fatigue strength criterion. The direct relation of physical damage to fatigue life and analytical equations for calculating residual elastic moduli  $E_1$ ,  $E_2$ ,  $\nu_{12}$  and  $G_{12}$  in terms of fatigue load and fatigue cycles are proposed. All proposed models in this thesis are analytical and general. The proposed approach enables prediction of fatigue behaviour of general laminates using experimental data of a basic lay-up such as unidirectional laminate. The analytical results have good agreement with four sets of experimental data. Based on the moduli reduction model developed by this research and O'Brien's delamination law, the finite element technique was utilized to model the fatigue failure process of notched laminates. A simple example of a laminate with a central hole under tension-tension fatigue loading was performed, and the results of damage growth and fatigue failure life approximately agree with experimental data.

## RÉSUMÉ

Cette recherche fait l'objet de l'étude de la fatigue des plaques de matériaux composites soumises à des chargements. La prédiction de l'amorce de la propagation des fissures matricielles et les délaminations sont étudiées en termes de tolérance aux endommagements, de dégradation du module d'élasticité, ainsi que de la dégradation de la résistance résiduelle. L'initiation de l'endommagement est prédit par un critère d'énergie des contraintes qui prend en compte les effets interactifs entre les fissures matricielles et les délaminations. En prenant comme hypothèse une relation linéaire entre le dommage et la perte du module d'élasticité, le développement de modèles permet de prédire la dégradation de la rigidité, les fissures matricielles et les délaminations en fonction de l'intensité du chargement et le nombre de cycles de l'épreuve de fatigue. Il y a quatre choix pour prédire la durée de vie utile en fatigue: un critère de module d'élasticité résiduel, un critère de fissures matricielles, un critère basé sur la dimension caractéristique de la délamination et un critère de résistance résiduelle. Une relation directe entre le dommage réel et la durée de vie utile en fatigue est proposée ainsi que des équations pour le calcul de propriétés caractéristiques résiduelles de matériaux ( $E_1$ ,  $E_2$ ,  $\nu_{12}$  et  $G_{12}$ ) en fonction du chargement et du nombre de cycles en fatigue. Ces modèles, étant analytiques et généraux, permettent de prédire le rendement de plaques composites, en utilisant des données expérimentales d'une configuration de base (par exemple, une plaque unidirectionnelle). C'est ainsi que les résultats ont montré un bon accord avec quatre expériences typiques sur des matériaux composites. A partir du modèle un code à éléments finis a été utilisé avec succès pour modéliser le comportement en fatigue d'une plaque percée d'un trou centrale.

## ACKNOWLEDGMENTS

The author wishes to express his deepest sincere gratitude and appreciation to my supervisor, Dr. Larry B. Lessard, for his enthusiasm, generosity, keen interest, excellent advice and constant guidance throughout the research program.

The author is indebted to his wife, Haiou, for her support, patience and understanding throughout the past two years.

## TABLE OF CONTENTS

ABSTRACT .....	i
RESUME .....	ii
ACKNOWLEDGMENTS .....	iii
TABLE OF CONTENTS .....	iv
LIST OF SYMBOLS .....	vii
LIST OF FIGURES .....	x
LIST OF TABLES .....	xiii

### CHAPTER 1 INTRODUCTION

1.1 Background .....	1
1.2 A review of fatigue failure mechanisms of composite laminates .....	3
1.2.1 Matrix cracking .....	5
1.2.2 Delamination .....	7
1.2.3 Change of modulus and strength .....	9
1.2.4 Notched composite laminates .....	11
1.3 A review of fatigue analysis methods of composite laminates .....	12
1.4 Objective .....	14

### CHAPTER 2 STIFFNESS LOSS DUE TO MATRIX CRACKING AND DELAMINATION

2.1 Stiffness loss in terms of matrix crack density .....	16
2.1.1 Stiffness loss in cross-ply laminates .....	16
2.1.2 Stiffness loss in general laminates .....	17
2.2 Stiffness loss in terms of delamination area .....	19

---

**CHAPTER 3 STIFFNESS DEGRADATION AND FATIGUE  
DAMAGE MODELS**

3.1 Damage variable and strain failure criterion .....	22
3.2 Fatigue stiffness degradation model .....	24
3.3 Bi-directional fatigue loading .....	26
3.4 Determination of constants, B, b and K .....	27

**CHAPTER 4 ONSET OF EDGE DELAMINATION AND  
MATRIX CRACKING**

4.1 Strain energy release rate due to matrix cracking .....	34
4.2 Strain energy release rate due to delamination .....	36
4.3 Total strain energy release rate .....	37

**CHAPTER 5 FATIGUE LIFE PREDICTION**

5.1 Fatigue life prediction in terms of matrix crack density .....	38
5.2 Fatigue life Prediction in terms of delamination area .....	39
5.3 Fatigue life prediction in terms of residual stiffness .....	39
5.3 Fatigue life prediction in terms of fatigue strength curve .....	40

**CHAPTER 6 EXAMPLES**

6.1 Cross-ply E-glass/epoxy laminate .....	42
6.2 $[\pm 45/0/90]_s$ E-glass/epoxy laminate .....	43
6.3 $[0/\pm 45]_s$ E-glass/epoxy laminate .....	44
6.4 $[0/90/\pm 45]_s$ T300/5208 laminate .....	44
6.5 Fatigue strength curves .....	45

**TABLE OF CONTENTS** **VI**

---

6.6 Summary ..... 45

**CHAPTER 7 NOTCHED LAMINATES UNDER CYCLIC LOADING**

7.1 Overview of finite element method for composite laminate ..... 50  
7.2 Calculation of residual moduli under bi-directional cyclic loading ..... 53  
7.3 Fatigue analysis by using the finite element technique ..... 55  
7.4 Example ..... 57  
7.5 Summary ..... 59

**CHAPTER 8 CONCLUSIONS AND RECOMMENDATIONS**

**REFERENCES** ..... 69

**APPENDIX A. RESIDUAL MODULI AND CRACK DENSITY** ..... 72

**APPENDIX B. ONSET OF LOCAL DELAMINATION** ..... 79

**APPENDIX C. COMPUTER CODES** ..... 84

---

**LIST OF SYMBOLS**

$a$	delamination length
$A$	total crack area
$A^0$	delamination area
$A^*$	total interfacial area
$B$	dimensionless constant for stiffness degradation
$b_0$	parameter of S-N curve of a unidirectional laminate
$b$	parameter of S-N curve of a general laminate
$C_m, C_d$	dimensionless constants for crack density and delamination area
$D$	global damage variable, dimensionless
$D_m$	crack damage variable, dimensionless
$D_a$	delamination damage variable, dimensionless
$D_f$	critical global damage variable
$E$	stiffness of a damaged composite laminate
$E_0$	stiffness of a undamaged composite laminate
$E_f$	fatigue failure stiffness
$E^*$	stiffness of a completely delaminated laminate
$E_{ld}$	modulus of delaminated region in the vicinity of matrix crack
$E_1, E_2, \nu_{12}, G_{12}$	residual elastic moduli of a laminate
$E_1^0, E_2^0, \nu_{12}^0, G_{12}^0$	initial elastic moduli of a laminate

---

$F_s$	safety factor
$G$	total strain energy release rate
$G_m$	strain energy release rate due to matrix cracking
$G_d$	strain energy release rate due to edge delamination
$G_c$	static critical strain energy release rate
$K_0$	parameter of S-N curve of a unidirectional laminate
$K$	parameters of S-N curve of a general laminate
$K_m$	crack density
$k_3, k_7$	material parameters relating to crack density
$k_{11}, k_{13}$	material parameters relating to crack density
$L$	length of a specimen
$m$	material parameter used in equation of the strain energy release rate
$n$	number of local delaminated plies
$N$	number of cycles
$N_f$	fatigue failure life
$P$	applied load
$q$	dimensionless failure factor
$R$	stress ratio, rate of maximum fatigue stress to minimum fatigue stress
$s$	crack spacing
$t_d$	thickness of delaminated region in the vicinity of matrix crack
$t$	thickness of a laminate
$t_c$	thickness of first failed ply

---

$V$	laminare volume
$W$	width of specimen
$\epsilon$	resultant strain
$\epsilon_u$	static ultimate strain
$\epsilon_f$	fatigue failure strain
$\epsilon_c$	critical strain for the onset of matrix cracking or delamination
$\theta$	fiber angle of cracked plies oriented to the direction of loading
$\sigma_{max}$	maximum applied fatigue cyclic stress
$\sigma_{ls}$	laminare static strength, determined by last ply failure theory
$\sigma_{0s}$	unidirectional laminare static strength
$\sigma_u$	laminare static ultimate strength, $\sigma_u = \sigma_{ls} / F_s$
$[G_c]$	element stiffness matrix
$[G_m]$	material moduli matrix
$[\nu]$	transforming matrix
$\{f\}$	vector of membrane force per unit length
$\{m\}$	vector of bending moments per unit length
$\{q\}$	vector of shear force per unit length
$\{x\}$	vector of curvatures
$\{\epsilon_m\}$	vector of membrane strain
$\{\gamma\}$	vector of transverse shear strain

## LIST OF FIGURES

Fig. 1.1	Depiction of damage modes: (a) matrix cracking with delamination, (b) matrix cracking, (c) fiber breakage with some fiber matrix debonding ...	4
Fig. 1.2	Development of damage in composite laminates under fatigue loading ...	4
Fig. 1.3	Micrographs showing crack patterns under fatigue loading in a $[0/90/\pm 45]_s$ laminate .....	6
Fig. 1.4	Fatigue cycles versus number of cracks for $[0/90/\pm 45]_s$ and $[0/\pm 45/90]_s$ laminates .....	7
Fig. 1.5	X-ray pictures of delamination growth as a function of fatigue cycles for a $[0/90/\pm 45]_s$ CFRP T300/5208 laminate .....	8
Fig. 1.6	S-N curves for various AS4/Epoxy laminates .....	10
Fig. 1.7	S-N curves for three CFRP T300/Epoxy laminates .....	10
Fig. 1.8	Change in modulus as a function of fatigue loading .....	11
Fig. 2.1	Rule of mixtures analysis of stiffness loss .....	20
Fig. 3.1	Fatigue and static strength normalized with respect to the unidirectional tensile strength .....	28
Fig. 4.1	Matrix cracking in a laminate .....	35
Fig. 6.1	Description of the problem .....	41
Fig. 6.2	Variation of the longitudinal stiffness and crack damage versus fatigue cycles for a $[0/90]_s$ laminate .....	46

Fig. 6.3	Variation of the longitudinal stiffness and crack damage versus fatigue cycles for a $[\pm 45/0/90]_s$ laminate .....	46
Fig. 6.4	Variation of the longitudinal stiffness versus fatigue cycles for a $[0/\pm 45]_s$ laminate .....	47
Fig. 6.5	Variation of the longitudinal stiffness versus fatigue cycles for a $[0/90\pm 45]_s$ T300/5208 laminate .....	47
Fig. 6.6	Fatigue strength versus number of cycles for $[0/90]_s$ , $[\pm 45/0/90]_s$ , $[0/\pm 45]_s$ glass/epoxy and $[0/90/\pm 45]_s$ T300/5208 graphite/epoxy laminates .....	48
Fig. 7.1	Flow chart of fatigue analysis process in notched laminated plate using the finite element method .....	56
Fig. 7.2	Description of the problem .....	60
Fig. 7.3	Finite element model of the problem .....	60
Fig. 7.4	Graphical representation of damage growth of a $[0/90/\pm 45]_s$ T300/5208 graphite/epoxy laminated plate under fatigue loading ( $\sigma_{\max} = 0.8 \sigma_{\text{ult}} = 218.5 \text{ MPa}$ , $R = 0.1$ ) .....	61
Fig. 7.5	Radiographs of damage growth in a $[0/90/\pm 45]_s$ T300/5208 graphite/epoxy laminated plate under fatigue loading ( $\sigma_{\max} = 0.8 \sigma_{\text{ult}} = 218.5 \text{ MPa}$ , $R = 0.1$ ) .....	63
Fig. A1.	A solid containing two sets of parallel cracks .....	72
Fig. A2.	A cross-ply laminate with cracks in the $90^\circ$ ply .....	75
Fig. A3.	Cracks in two plies symmetrically placed about the $X_1$ axis .....	76
Fig. B1.	Depiction of local delamination growing from matrix cracks .....	80

**LIST OF FIGURES**

---

**Fig. B2.** Model of local delamination ..... 80

**Fig. B3.** Strain energy release rate at delamination onset as function of  
fatigue cycles ..... 83

**Fig. B4.** Strain energy release rate at delamination onset as function of fatigue cycles  
for X751/50 E-glass/epoxy ..... 83

---

**LIST OF TABLES**

Table 1. Material properties of three E-glass/epoxy and one graphite/epoxy laminates .....	42
Table 2. Material properties for a $[0/90/\pm 45]_s$ T300/5208 specimen .....	57

# CHAPTER 1

## INTRODUCTION

In this chapter, the history and background of fatigue failure mechanisms for composite materials are briefly described. The analysis methods and recent developments related to structures made of composite laminates under fatigue loading are reviewed. The objectives of this research work are presented.

### 1.1 BACKGROUND

The rapidly expanding applications of composites in the recent past have provided much optimism for the future of technology. Although man-made composites have existed for thousands of years, high technology of composites has evolved in the aerospace industry only in the last twenty years. Filament-wound pressure vessels using glass fibers were the first strength critical application for modern composites. This was followed by boron filaments in the 1960's which started many US Air Force programs to promote aircraft structures made of composites. The F-111 horizontal stabilizer in the early 1970's was the first important flight-worthy composite component.

In the early 1980's the Boeing 767 used nearly two tons of composite materials in its floor beam and all of its control surfaces. The USSR's giant transport, Antonov 124, has a total of 5500 kg of composite materials, of which 2500 kg are graphite composites. The all-composite fin box of the Airbus industries A310-300 is an impressive structure in its simplicity. Nearly all emerging aircrafts use composites extensively; examples include the Dassault-Breguet's Rafale, Saab-Scania JAS-39 Gripen, the European Fighter Aircraft of Britain, West Germany, Canada, Italy and

Spain, and a new generation of commercial aircraft: Airbus 320, McDonnell-Douglas MD-11, and Boeing 7J7. Beech Aircraft's Straship-1 is an all-composite airplane.

In 1986, another all-composite airplane that set a world record for nonstop flight around the world was the VOYAGER designed and built by Burt Rutan and his coworkers. As expected the plane was ultra light but it also showed amazing toughness and resilience against many stormy encounters. Graphite composites were used in the dual rudders of the revolutionary 12-meter yacht, the USA, St. Francis Yacht Club's entry to the 1987 America's Cup challenge. From the 1980's to 1990's more and more applications have converted composite materials from a high technology domain into household words. High visibility is an important ingredient for the growth and acceptance of composite materials as viable engineering materials.

Materials and processing advances have been instrumental to the growth of our technology. Graphite and Kevlar fibers became commercially available in the early 1970's. More recently, higher temperature materials and thermoplastics have emerged for the demanding applications of the future.

The high technology of composites has spurred applications outside the aerospace industry. The sporting goods industry is a major outlet for composite materials. Hundreds of tons of graphite composites were used for tennis and squash rackets, and golf shafts each year since 1983. Other applications include bicycles, oars for rowing, and just about any equipment where weight, stiffness, and strength are important. It is believed that the acceptance of composites will inevitably increase because of their inherent high specific strength and specific stiffness and superior long term properties.

## 1.2 FATIGUE FAILURE MECHANISMS

Composite materials exhibit very complex failure mechanisms under static and fatigue loading because of anisotropic characteristics in their strength and stiffness properties. Fatigue failure is usually accompanied with extensive damage which is multiplied throughout specimen volume instead of a predominant single crack which is often observed in most isotropic brittle materials. The four basic failure mechanisms for composites under fatigue loading are matrix cracking, interfacial debonding (fiber/matrix debonding), delamination and fiber breakage. Figure 1.1 and Figure 1.2 represent basic damage modes and development of damage in composite laminates under fatigue loading. Any combination of these can be responsible for fatigue damage which may result in reduced fatigue strength and stiffness. The type and degree of damage vary widely depending on material properties, lay-up of the composite plies, type of fatigue loading, etc. It has also been observed that damage development under fatigue and static loading is similar except that fatigue at given stress level causes additional damage to occur as a function of number of cycles.

Although four basic failure mechanisms have been observed in composites, many researchers have indicated that delamination and matrix cracking are the main observed modes of fatigue failure before a composite laminate fails catastrophically, and both have significant effect on laminate stiffness and strength. Figure 1.1 (a) shows idealized schematics of fatigue damage mechanisms for matrix cracking and delamination.

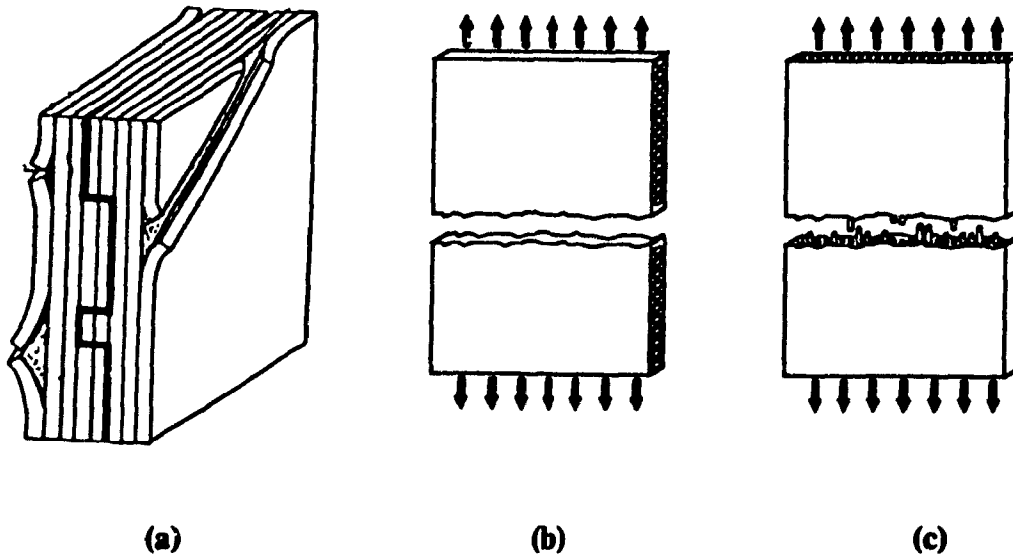


**Fig. 1.1** Depiction of damage modes: (a) matrix cracking with delamination, (b) matrix cracking, (c) fiber breakage with some fiber matrix debonding [1,2].

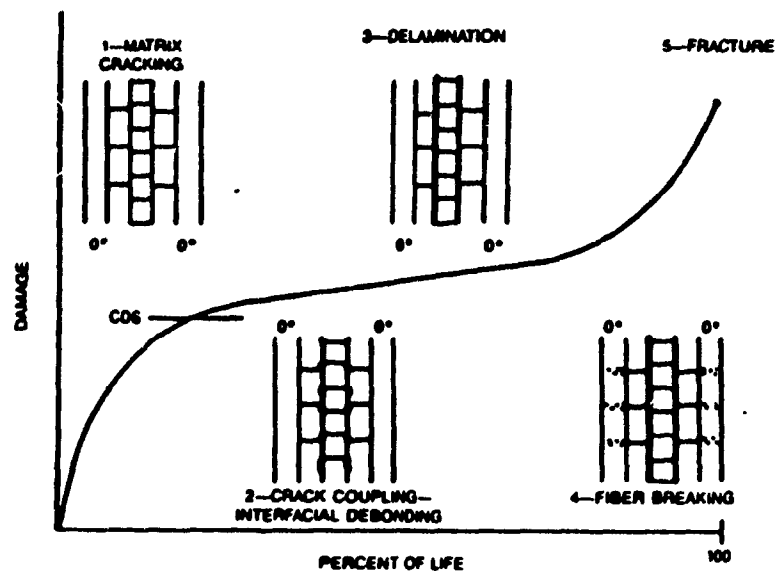
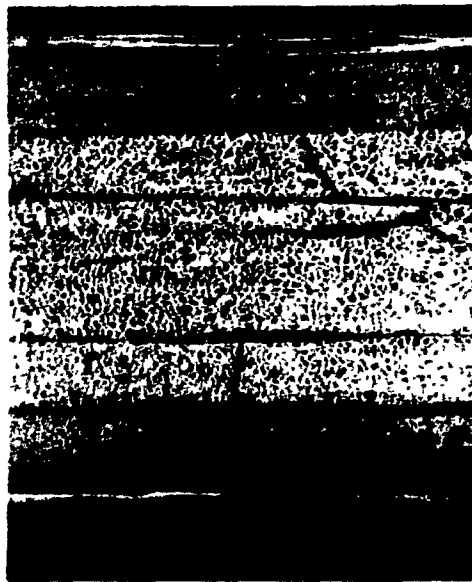


**Fig. 1.2** Development of damage in composite laminates under fatigue loading [3]

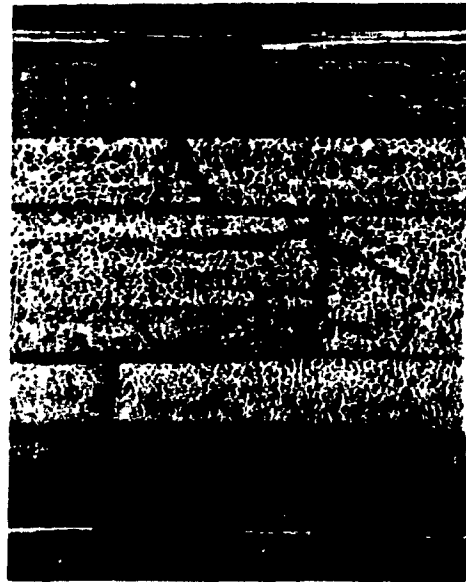
### 1.2.1 Matrix cracking

For multidirectional laminates under in-plane fatigue loading, failure usually occurs successively from the weakest ply to the strongest ply. As an example, consider the matrix cracking process of a  $[0/90/\pm 45]_s$  laminate subjected to uniaxial tension. It would be expected that the first cracks occur in 90 degree plies followed by  $\pm 45$  degree plies. Figure 1.3 presents a series of micrographs of transverse cracks observed at free edges during fatigue loading. First cracks occurred in the 90 degree plies and propagated to the interfaces. With increasing fatigue cycles, new cracks occurred in the 45 degree plies adjacent to the 90 degree plies, and then to the -45 degree plies. Most of these cracks appear at the tip of the 90 degree cracks and are extended to the interface of the  $\pm 45$  degree plies. In fatigue loading, the number of cracks in each angle ply is higher compared to that of static loading and increases with fatigue cycles. However, prior to laminate failure the number of cracks in most cases reaches a limit level where no further new cracks occur in spite of additional fatigue cycles. The stress level of onset of matrix cracking during fatigue loading in the  $[0/90/\pm 45]_s$  laminate was also found to be much smaller than that of onset of matrix cracking under static load. Thus, the first ply failure criterion at static load is not valid for fatigue load.

The laminate stacking sequence plays a significant role in the development of matrix cracks [4]. Although the same stress state was predicted for different plies of same or similar laminates by laminate plate theory, different matrix crack densities are often observed in these plies or laminates under fatigue loading. Figure 1.4 shows fatigue cycles versus number of cracks for  $[0/90/\pm 45]_s$  and  $[0/\pm 45/90]_s$  laminates. There is a considerable difference in the development of 90 degree and  $\pm 45$  degree cracks between two stacking sequences of a quasi-isotropic laminate, as well as in the development of +45 degree and -45 degree cracks within the  $[0/90/\pm 45]_s$  laminate. The main reason for this discrepancy is the redistribution of ply stresses due to matrix crack growth and ply delamination.



(a)  $2 \times 10^4$  CYCLES



(b)  $4 \times 10^4$  CYCLES



(c)  $20 \times 10^4$  CYCLES



(d)  $65 \times 10^4$  CYCLES

**Fig. 1.3** Micrographs showing crack patterns under fatigue loading in a  $[0/90/\pm 45]_s$  laminate [4]

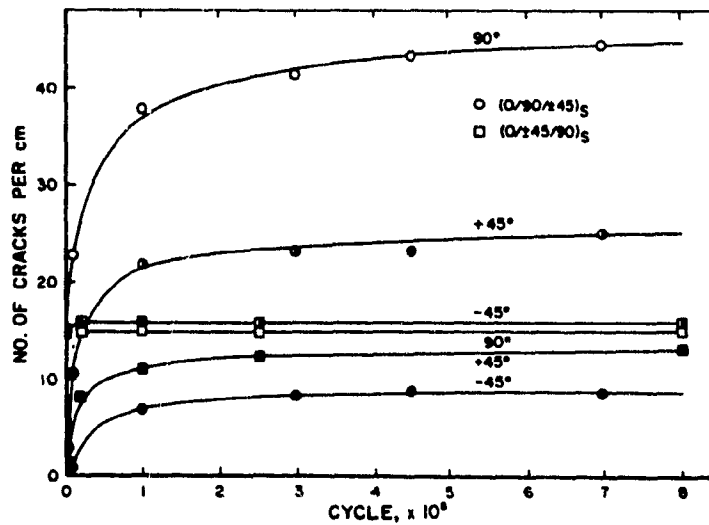


Fig. 1.4 Fatigue cycles versus number of cracks for  $[0/90/\pm 45]_s$  and  $[0/\pm 45/90]_s$  laminates [4]

### 1.2.2 Delamination

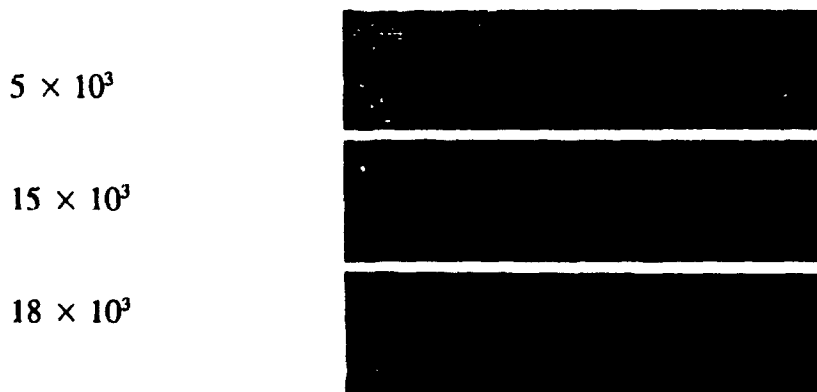
Delamination along the straight free-edges of composite laminates under in-plane uniaxial load has been observed since the early 1970's. Since then a considerable amount of work has been reported on the free-edge problem in composite materials [2,4,5,6], which indicate that free-edge delamination is attributed to the existence of interlaminar stresses which are highly localized in the neighborhood of a free-edge. In addition to interlaminar tensile stress, other mechanisms such as transverse cracking and interlaminar shearing are also significant in the onset and growth of delamination.

Figure 1.5 shows a x-ray picture of delamination growth as a function of number of cycles for a  $[0/90/\pm 45]_s$  CFRP T300/5208 laminate. The stress level of delamination during fatigue loading is smaller than that of delamination under static loading. Onset of delamination occurred very early in the fatigue life and rapidly propagated toward the middle of the specimen width as number of cycles was increased.



(a)  $\sigma_{\max} = 345 \text{ MPa}$

$N = 312,000 \text{ CYCLES}$



(b)  $\sigma_{\max} = 414 \text{ MPa}$

$N = 19,000 \text{ CYCLES}$

**Fig. 1.5** X-ray pictures of delamination growth as a function of fatigue cycles for a  $[0/90/\pm 45]_s$  CFRP T300/5208 laminate [4]

### 1.2.3 Change of modulus and strength

Fatigue damage, such as matrix cracking and delamination, often results in a significant reduction in modulus and strength of composite laminates. A multidirectional laminate generally shows a gradual strength and modulus reduction until final failure. The degree of modulus and strength reduction varies widely, depending upon the lay-up of laminate, type of loading, material properties, etc.

Figure 1.6 and Figure 1.7 show the S-N curves for CFRP AS4/3502 and T300/5208 laminates, respectively. The graphs represent fatigue cycles versus the fatigue strength ratio (ratio of fatigue stress to static strength). Laminates with matrix dominant failure modes exhibit a lower fatigue resistance than laminates with fiber dominant failure modes. The slope of the S-N curve tends to increase as the content of 0 degree plies decreases. The fatigue strength of a  $[\pm 45]_s$  laminate is frequently used to determine longitudinal shear fatigue strength [4].

Although initial static tensile and compressive strengths are almost equal to each other, strength reduction is much greater in tension than in compression. In most cases of compression-compression fatigue loading, no appreciable matrix damage is observed until final fatigue failure. Most compression failures are characterized by delamination and compression buckling. Figure 1.8 shows the change of modulus with fatigue cycles for various fatigue loadings. A significant modulus change is obvious in specimens subjected to tension-tension and tension-compression fatigue loading, whereas little or no modulus change is observed in compression-compression fatigue loading.

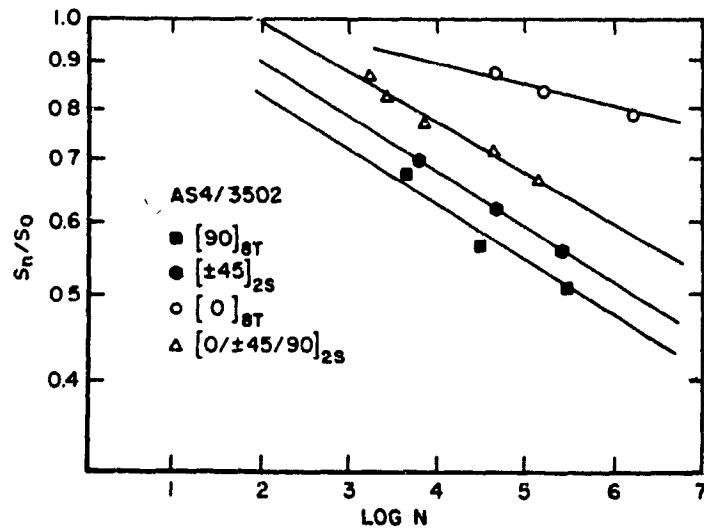


Fig. 1.6 S-N curves for various AS4/Epoxy laminates [4]

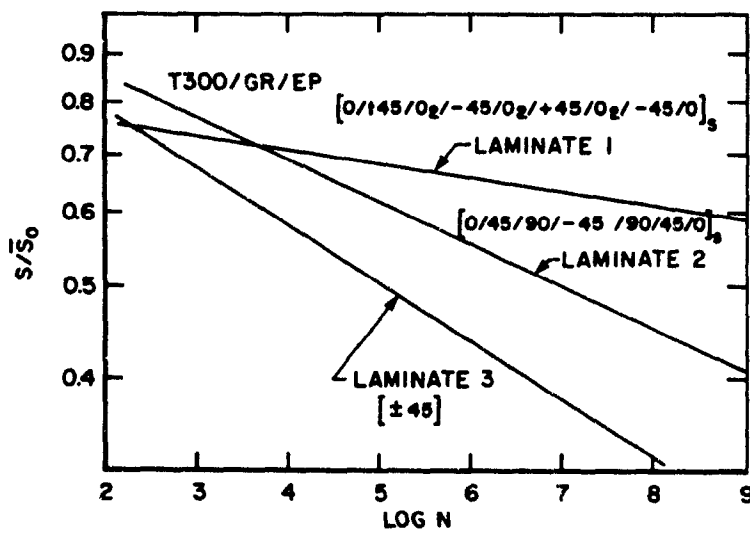


Fig. 1.7 S-N curves for three CFRP T300/Epoxy laminates [4]

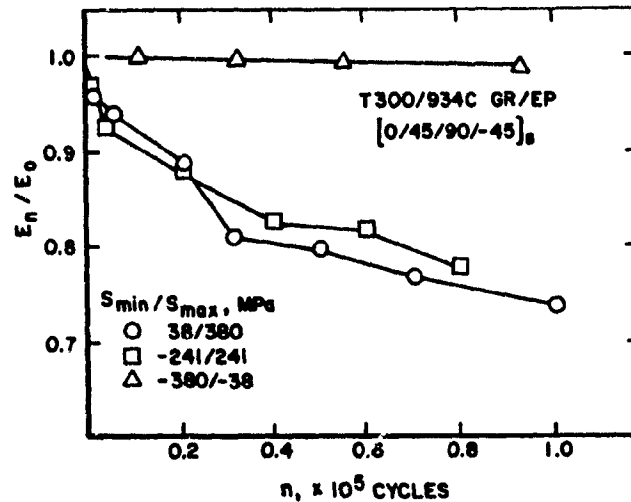


Fig. 1.8 Change in modulus as a function of fatigue loading [4]

#### 1.2.4 Notched composite laminates

An important aspect of fatigue analysis of composite materials is the behavior of laminates with geometric discontinuities such as holes, joints, ply terminations, and inherent defects. The performance of these notched laminates under fatigue loading is controlled by the stress fields and material performance in the neighborhood of stress concentrators, the most common being a joint or access hole. Fatigue data for most composite laminates indicate that reduction of fatigue strength resulting from the presence of small notches, compared to unnotched specimens, is found to be insignificant. The excellent fatigue resistance of notched specimens is mainly due to types of damage which relax the stress concentration around the notch tips.

For the case of the presence of large notches, the effect of notches on fatigue

strength is more significant and must be rigorously investigated. In metals, the problem of stress concentration resulting from various notches is well defined by the many stress concentration factors which influence the behavior under cyclic stress and the crack propagation is easily related to specimen data through the use of fracture mechanics. In notched composite laminates, however, the damage modes and growth around notches are seen to be quite different. Multiple cracks coupled with delamination are often observed in the region around notches where combined stresses are produced that vary widely around the notch during the fatigue life of the laminate. When damage occurs, changes of moduli around the notch result in changes of magnitude and redistribution of stresses. The subsequent stress analysis becomes very difficult because the relation of residual moduli to cyclic load and number of cycles is very complex. The stress redistribution after fatigue damage has made it difficult to predict the fatigue strength of notched laminate using the fatigue strength of the unnotched specimens.

### **1.3 A REVIEW OF FATIGUE ANALYSIS METHODS OF COMPOSITE LAMINATES**

The prediction of fatigue damage and fatigue life for composite materials has been the focus of many investigations during the past two decades. Because composite laminates exhibit very complex matrix cracking and delamination accumulation processes, up to now, the models proposed by many investigators for composite laminates under fatigue loading have been limited to particular laminates and strongly dependent on experimental data. The residual strength degradation, modulus degradation, and damage tolerance approaches are the main methods which have been used to study fatigue damage and to predict fatigue life of composites.

In the residual strength degradation approach, the residual strength is gradually reduced and fatigue failure occurs when residual strength equals the maximum applied

stress. Broutman and Sahu [7] proposed a cumulative damage theory using a linear strength degradation equation. Hahn and Kim [8] introduced a nonlinear residual strength degradation equation which assumes that the slope of the residual strength is inversely proportional to some power of the residual strength itself. This nonlinear degradation model was investigated further by Yang and Liu [9] for the purpose of reliability study in fatigue life of composite materials. Charewize and Daniel [10] proposed a damage model based on the assumption that the residual strength degradation rate is a function of life fraction, but not a function of residual strength. An advanced residual strength degradation model which can predict single- and multi- stress level fatigue life of composite laminate was proposed by Reifsnider and Stinchcomb [11], based on the assumption that the residual strength degradation rate is a power function of fatigue cycles  $N$ . After setting up basic equations, they modified them by defining a critical element and introducing a local failure function deduced from microstructural analysis in composite laminates.

In the modulus degradation approach, the modulus is gradually reduced and fatigue failure occurs when the modulus degrades to a certain level. The critical level of modulus degradation has been defined by many investigators. "Failure occurs when the fatigue secant modulus degrades to the static secant modulus" was proposed by Hahn and Kim [12] and by O'Brien and Reifsnider [13]; "Failure occurs when the fatigue resultant strain reaches the static ultimate strain" was suggested by Hwang and Han [5]. This is an indirect definition of the modulus degradation criterion. O'Brien [2,6,14] proposed a simple analytical model to predict modulus degradation due to delamination by using a rule of mixtures in conjunction with laminate plate theory. Based on shear-lag analysis, the modulus degradation as function of matrix crack density in cross-ply laminates was predicted by [15] and [16]. Beaumont [17], analogous to fracture mechanics, proposed an equation for evaluating residual stiffness as function of applied stress and fatigue cycles for cross-ply laminates. Talreja [3], based on cracked laminate elastic theory and assuming that elastic strain energy is a function of the strain tensor and

damage vector, derived a set of equations to calculate residual elastic moduli as function of matrix cracks.

The theory and analysis method of damage tolerance for composite materials were developed by O'Brien [2]. Fatigue failure was defined such that it will occur if the maximum global strain, resulting from the stiffness loss associated with damage growth at a certain number of fatigue cycles, reaches the effective failure strain when the local delamination forms. This approach combined both residual strength degradation and modulus degradation by using the concept of strain energy release rate and a delamination growth law. The fail-safety was assessed by accounting for the accumulation of delamination through the thickness.

All above theories and approaches were verified by fatigue tests and have good agreement with test results. However, the validity of analytical equations more or less depends upon the particular laminates tested, implying that the equations are no longer valid if material properties, laminate lay-up or direction of fatigue loading is changed, i.e., the solutions are not general. The direct relation of physical damage such as matrix cracking and delamination to fatigue life and analytical equations for predicting physical damage in terms of fatigue load and fatigue cycles for general laminates have not been found.

## **1.4 OBJECTIVE**

The prediction of fatigue life and evaluation of onset and growth of matrix cracking and delamination for general notched and unnotched composite laminates will be studied analytically. Based on the analysis of damage tolerance, residual modulus and residual strength, a new and more generalized analytical approach will be proposed for

the fatigue response of composite laminates to cyclic loading. The objectives of the proposed approach are to obtain the following information:

1. The onset and growth as well as type of damage in general laminates as a function of fatigue stress and number of loading cycles.
2. The effect of physical damage on stiffness, strength, and life of the laminate.
3. The fatigue behavior relationship between general laminates and unidirectional laminates.
4. The prediction of fatigue behavior of a laminate with a central hole subjected to tension-tension cyclic load using the finite element technique.

## **CHAPTER 2**

### **STIFFNESS LOSS DUE TO MATRIX CRACKING AND DELAMINATION**

The models of stiffness loss as function of matrix crack density and delamination size are reviewed and developed in this chapter. Based on models by Talreja [3] and O'Brien [6], a fundamental assumption that stiffness loss under static and fatigue load can be characterized approximately by a linear relation with matrix crack density and delamination area is proposed.

#### **2.1 STIFFNESS LOSS IN TERMS OF MATRIX CRACK DENSITY**

##### **2.1.1 Stiffness loss in cross-ply laminates**

In composite laminates, fatigue failure such as matrix cracking is usually accompanied with extensive damage which is multiplied throughout specimen volume instead of a predominant single crack which is often observed in most isotropic brittle materials. Composite laminates exhibit very complex matrix crack accumulation processes due to redistribution of ply stress at ply interfaces. Although the same stress state is predicted for different plies by laminate plate theory, different matrix crack densities at these plies are often observed for composite laminates under fatigue load. For the specific case where matrix cracking is the dominant mode of failure such as in a cross-ply laminate, O'Brien [6, 16] and Beaumont [17], based on a shear-lag analysis, suggested a stiffness degradation model as a function of matrix crack spacing,  $s$ , which was expressed as

$$\frac{E}{E_0} = \frac{1}{1 + \frac{E_0}{E_1} \left( \frac{b+d}{b} - \frac{E_1}{E_0} \right) \frac{\tanh(ws)}{ws}} \quad (1)$$

where  $b$  and  $d$  are the thickness of the longitudinal and transverse plies, respectively.  $E_1$  and  $E_2$  are the Young's modulus of the longitudinal and transverse plies.  $E$  and  $E_0$  are stiffness of the damaged and undamaged laminate, and  $w$  is constant expressed as

$$w^2 = \frac{3 G (b+d) E_0}{d^2 b E_1 E_2} \quad (2)$$

where  $G$  is the shear modulus in the longitudinal direction of the transverse ply. Equation (1) can, almost always, be approximated to give

$$\frac{E}{E_0} = 1 - C_m K_m \quad (3)$$

where  $K_m = 1/2s$  is the crack density and  $C_m$  is constant.

### 2.1.2 Stiffness loss in general laminates

If both matrix cracking and delamination occur in the composite laminate under cyclic loading and both have significant effect on fatigue damage, the development of a workable procedure for prediction of fatigue behavior, such as damage onset and growth, stiffness loss, fatigue failure life, etc., is very complex. Talreja [3], based on micromechanics and continuum damage theory and the assumption that elastic strain energy is a function of the strain tensor and crack damage vector, proposed a model to represent the relationship between residual stiffness and matrix crack density (see appendix A). After extension of Talreja's work, the proposed equations can be written as

$$\begin{aligned}
 E_1 &= E_1^0 + 2D_m[k_3 + k_7(v_{12}^0)^2 - k_{13}v_{12}^0] \\
 E_2 &= E_2^0 + 2D_m[k_7 + k_3(v_{21}^0)^2 - k_{13}v_{21}^0] \\
 v_{12} &= v_{12}^0 + D_m \left[ \frac{1 - v_{12}^0 v_{21}^0}{E_2^0} \right] (k_{13} - 2k_7 v_{12}^0) \\
 G_{12} &= G_{12}^0 + 2D_m k_{11}
 \end{aligned} \tag{4}$$

and

$$D_m = \sum_{i=1}^m \left( \frac{K_{mi}}{\sin \theta_i} \frac{t_i^2}{t} \right) \tag{5}$$

where  $t_i$  is the thickness of the ply containing the cracks and  $t$  is the total thickness of laminate.  $K_{mi}$  and  $\theta_i$  are the crack density and orientation angle of the fiber at a cracked ply, respectively. The moduli with superscript 0 refer to the uncracked laminate which is calculated by laminate plate theory.  $k_3$ ,  $k_7$ ,  $k_{11}$  and  $k_{13}$  are materials constants and are given by appendix A.

The first line of equation (4) can be expressed by

$$\frac{E_1^0 - E_1}{E_1^0} = -D_m \frac{2[k_3 + k_7(v_{12}^0)^2 - k_{13}v_{12}^0]}{E_1^0} \tag{6}$$

or

$$D = \frac{E_0 - E}{E_0} = 1 - \frac{E}{E_0} = C_m D_m \tag{7}$$

where

$$C_m = -\frac{2[k_3 + k_7(v_{12}^0)^2 - k_{13}v_{12}^0]}{E_1^0} \quad (8)$$

$D$  in equation (7) may be called "global damage variable" and  $D_m$  may be called "crack damage variable."  $C_m$  is a dimensionless constant which depends on material properties and laminate lay-up. Equation (7) characterizes the effect of total matrix cracks in the laminate on stiffness degradation and reduces to the form of equation (3) for the specific case of a cross-ply laminate.

## 2.2 STIFFNESS LOSS IN TERMS OF DELAMINATION AREA

Stiffness loss due to delamination depends on the laminate lay-up and the material properties of the fiber and matrix, as well as the location and extent of the delamination. The laminate stiffness decreases as delamination forms and grows at a particular interface. O'Brien [6] proposed an analytical equation for the stiffness loss associated with edge delamination as

$$E = (E^* - E_0)\frac{a}{b} + E_0 \quad (9)$$

Where  $a/b$  is the ratio of the delamination size to the laminate half-width,  $E_0$  is undelaminated laminate stiffness, and  $E^*$  is the stiffness of a laminate completely delaminated along one or more interfaces, which is calculated by the rule of mixtures, i.e.,

$$E^* = \sum_{i=1}^m \frac{E_i t_i}{t} \quad (10)$$

where (see Figure 2.1)

$m$  = number of sublaminates formed by the delamination.

$E_i$  = the laminate stiffness of the  $i$ th sublaminates formed by the delamination.

$t_i$  = the thickness of the  $i$ th sublaminate

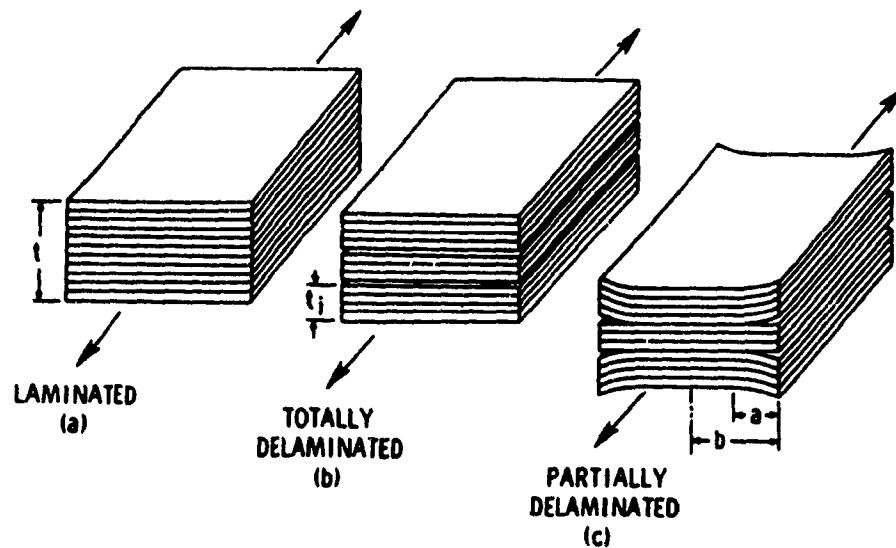


Fig. 2.1 Rule of mixtures analysis of stiffness loss [6]

A more general form of equation (9) may be developed by assuming that the relationship between laminate stiffness loss and delamination area can be represented by

$$\frac{E-E_0}{E^*-E_0} = \frac{A^0}{A^*} \quad (11)$$

Equation (11) can be rewritten as

$$D = 1 - \frac{E}{E_0} = C_d D_d \quad (12)$$

where

$$C_d = \frac{E_0 - E^*}{E_0} \quad ; \quad D_d = \frac{A^0}{A^*} \quad (13)$$

and

$A^0$  = delaminated area

$A^*$  = total interfacial area

The  $D_d$  in equation (12) may be called the "delamination damage variable" and  $C_d$  is a dimensionless constant. Equation (12) characterizes the stiffness loss due to delamination.

Based on equation (7) and equation (12), it is reasonable to make an assumption that stiffness loss can be characterized approximately by a linear relation with matrix crack density or delamination area for general composite laminates. However, the prediction of stiffness loss as a function of fatigue load and number of fatigue cycles for general laminates is very complex. In this research a workable approach is proposed and will be discussed.

## **CHAPTER 3**

# **STIFFNESS DEGRADATION AND FATIGUE DAMAGE MODELS**

Following Chapter 2, another fundamental assumption is proposed, which states that global damage growth rate  $dD/dN$  is proportional to some power of applied fatigue stress and inversely proportional to some power of current level of the damage variable  $D$  itself. The analytical models of modulus degradation, matrix crack density and delamination area growth in terms of fatigue stress and number of cycles is derived, which allows prediction of fatigue damage of composite laminates with arbitrary lay-up, using a minimum of experimental measurement.

### **3.1 DAMAGE VARIABLE AND STRAIN FAILURE CRITERION**

The selection of damage variable should take account of the following considerations:

1. The damage variable should have a direct physical meaning or be directly related to physical quantities which are easy to measure;
2. The damage variable should phenomenologically describe the physical process of damage accumulation and correlate well with damage state in composite materials.

From the above analysis of delamination and matrix cracking, comparing equation (7) and equation (12), it is reasonable for us to select global damage variable  $D$  to predict matrix crack density and delamination size and to perform fatigue life analysis. Global damage variable  $D$  provides an indirect measurement of physical damage in composite laminates,

instead of direct measurement of delamination size and number of matrix cracks. It is clearly seen that  $D=0$  indicates a material state with no damage and catastrophic failure occurs when  $D$  is gradually increased to a certain critical level  $D_f$ . The value of  $D_f$  may be determined by using the well-known strain failure criterion.

The strain failure criterion is one of most widely used criterion for predicting fatigue life. The strain failure criterion states that final failure of material occurs when the fatigue resultant strain reaches the static ultimate strain [5]. Based on the elastic stress-strain relation under static loading, the following relation is obtained:

$$\sigma_u = E_0 \varepsilon_u \quad (14)$$

where  $\varepsilon_u$  is static ultimate strain and  $\sigma_u$  is static ultimate strength. The stress-strain relation under fatigue loading gives

$$\sigma_{max} = E_f \varepsilon_f \quad (15)$$

where  $\varepsilon_f$  and  $E_f$  are fatigue strain and fatigue modulus at failure under fatigue stress level  $\sigma_{max}$ , respectively. Using strain failure criterion ( $\varepsilon_u = \varepsilon_f$ ) and combining equation (14) and equation (15) gives the following relation :

$$\frac{E_f}{E_0} = \frac{\sigma_{max}}{\sigma_u} = q \quad (16)$$

and critical global damage variable  $D_f$  can be expressed by

$$D_f = 1 - \frac{E_f}{E_0} = 1 - q \quad (17)$$

where  $q$  may be called the "failure factor."

### 3.2 FATIGUE STIFFNESS DEGRADATION MODEL

In order to make following analysis clear, differentiate equation (7) and equation (12) to give

$$\frac{dD}{dN} = C_m \frac{dD_m}{dN} \quad (18)$$

$$\frac{dD}{dN} = C_d \frac{dD_d}{dN} \quad (19)$$

Many experimental observations report that the crack density growth rate  $dD_m/dN$  and delamination area growth rate  $dD_d/dN$  are directly proportional to some power of the fatigue stress and inverse proportional to the some power of current level of damage itself [6,17,18]. Based on the linear relation of global damage variable growth rate  $dD/dN$  with matrix crack density growth rate and delamination area growth rate (equation (18) and equation (19)), in this research it is assumed that the global damage variable growth rate,  $dD/dN$ , can be expressed by:

$$\frac{dD}{dN} = \frac{A \sigma_{\max}^C}{B D^{B-1}} \quad (20)$$

where A, B and C are unknown constants, N is number of cycles, and  $\sigma_{\max}$  is maximum fatigue stress. Integrating equation (20) and noting that  $D=0$  when  $N=0$  yields

$$D = (A N \sigma_{\max}^C)^{\frac{1}{B}} \quad (21)$$

Assuming that the S-N relation for a composite laminate under fatigue loading is given and can be represented by

$$K N_f \sigma_{\max}^b = 1 \quad (22)$$

where  $K$  and  $b$  are unknown constants, and  $N_f$  is fatigue failure life at maximum fatigue stress level  $\sigma_{\max}$ . Rewriting equation (21) gives

$$\frac{A}{D^B} N \sigma_{\max}^C = 1 \quad (23)$$

Comparing equation (22) with equation (23) and noting that  $D=D_f$  when  $N=N_f$  obtains

$$A = K D_f^B \quad ; \quad C = b \quad (24)$$

Substituting equation (17) into equation (24), then into equation (21) and noting that  $D = 1 - E/E_0$  yield

$$\frac{E}{E_0} = 1 - D = 1 - (K N \sigma_{\max}^b)^{\frac{1}{B}} (1-q) \quad (25)$$

Equation (25) can be used to evaluate stiffness loss for laminates under fatigue loading if constants,  $B$ ,  $b$  and  $K$ , are given. Based on equation (25), the relationship of matrix crack density and delamination area growth with fatigue load and fatigue cycles can be obtained by substitution of equation (25) into equation (12) and equation (7), that is, for delamination:

$$D_d = (K N \sigma_{\max}^b)^{\frac{1}{B}} \frac{(1-q)}{C_d} \quad (26)$$

and for matrix cracking:

$$D_m = (K N \sigma_{\max}^b)^{\frac{1}{B}} \frac{(1-q)}{C_m} \quad (27)$$

Equation (4) is repeated here

$$\begin{aligned}
 E_1 &= E_1^0 + 2D_m[k_3 + k_7(v_{12}^0)^2 - k_{13}v_{12}^0] \\
 E_2 &= E_2^0 + 2D_m[k_7 + k_3(v_{21}^0)^2 - k_{13}v_{21}^0] \\
 v_{12} &= v_{12}^0 + D_m\left[\frac{1 - v_{12}^0v_{21}^0}{E_2^0}\right](k_{13} - 2k_7v_{12}^0) \\
 G_{12} &= G_{12}^0 + 2D_mk_{11}
 \end{aligned} \tag{28}$$

$D_m$  is now related to number of fatigue cycles and fatigue load and is expressed by equation (27).

It should be stated that equations (25), (26) and (27) are only valid for predicting growth of fatigue damage. For the case of very low level fatigue stress or number of cycles, damage initiation should be determined before using the damage growth equations. The prediction of fatigue damage onset will be discussed in Chapter 4.

### 3.3 BI-DIRECTIONAL FATIGUE LOADING

The prediction of fatigue damage and fatigue life under multi-directional fatigue loads for general laminates is very complicated because of data scatter in fatigue experiments. The approach of using unidirectional fatigue test data to evaluate the fatigue failure for multi-directional fatigue loads needs to be developed further. For the specific cases of a laminate only subjected to bi-directional fatigue loads  $\sigma_1$  and  $\sigma_2$ , linear superposition of the effect of these two load components may be performed. For

example, a  $[0/90_2]_s$  cross-ply laminate subjected to loads in two directions  $\sigma_1$  and  $\sigma_2$  may be resolved into two cases, one is  $[0/90_2]_s$  laminate subjected to  $\sigma_1$  load in the direction of 0 degree fiber, and another is  $[90/0_2]_s$  laminate subjected to  $\sigma_2$  also in the direction of 0 degree fibre. The two cases are first calculated separately and then these results are added together by linear superposition. The application of this method to notched laminates will be discussed in Chapter 7.

### 3.4 DETERMINATION OF CONSTANTS, B, b, AND K.

The validation of equations (25),(26) and (27) is dependent on constants B, b and K, which are governed by material properties, laminate lay-up, types of loading, etc. These required constants can be obtained experimentally by using a regression analysis method and the form of equation (25). This is a direct and simple method, but the equations will lose generality because measured residual stiffness data is taken from particular laminates. An analytical method is proposed to calculate the above constants. Two assumptions must first be made, which are:

1. The ratio of laminate fatigue strength to unidirectional fatigue strength is approximately equal to that of laminate static strength to unidirectional static strength. This assumption is reasonable because both static strength and fatigue strength of the laminate are mainly dependent upon the percentage and strength of 0 degree plies. The damage development under fatigue and static loading are similar except that fatigue causes additional damage to occur as a function of number of fatigue cycles. Figure 3.1 shows this relationship for various laminates of CFRP T300/5208.
2. The form of equation (12) is also valid for local delamination. The validation of this assumption will become evident by the coming equation (37).

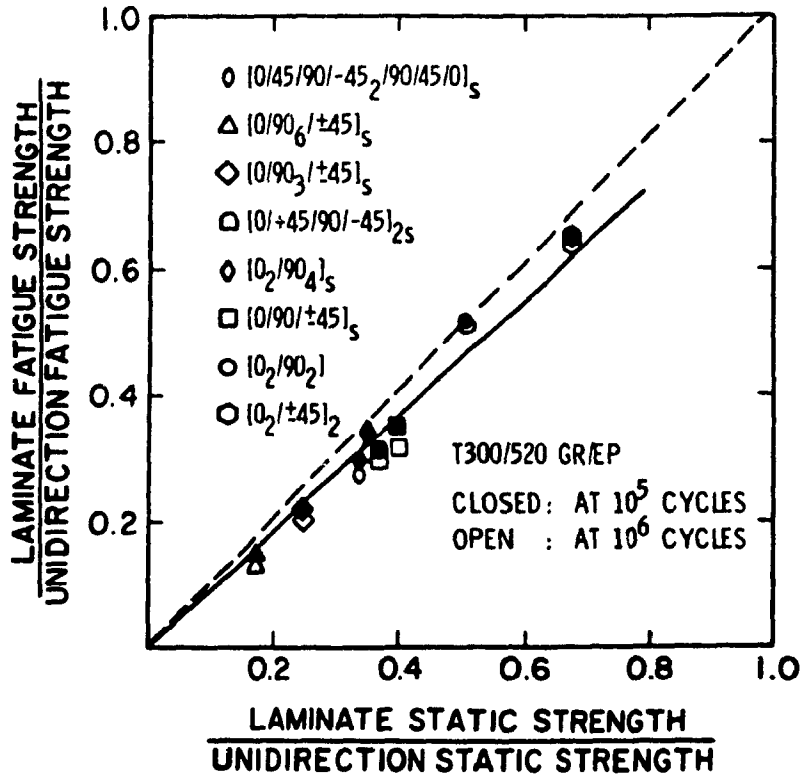


**Fig. 3.1** Fatigue and static strength normalized with respect to unidirectional tensile strength [4]

According to assumption 1, the ratio of laminate fatigue and static strength to unidirectional strength can be represented by

$$\frac{\sigma_{lf}}{\sigma_{of}} = \frac{\sigma_{ls}}{\sigma_{os}} \quad (29)$$

where

$\sigma_{lf}$  - laminate fatigue strength,

$\sigma_{of}$  - unidirectional fatigue strength, i.e. 0 degree laminate fatigue strength,

$\sigma_{ls}$  - laminate static strength,

$\sigma_{os}$  - unidirectional static strength, i.e., 0 degree laminate static strength.

Assuming the S-N relation for unidirectional laminate can be expressed by

$$K_0 N (\sigma_{0f})^{b_0} = 1 \quad (30)$$

where  $b_0$  and  $K_0$  are constants. Also assume that the S-N relation for a general laminate can be expressed by

$$K N (\sigma_f)^b = 1 \quad (31)$$

Combination of equation (30) and equation (31) gives

$$\frac{\sigma_f}{\sigma_{0f}} = \frac{(K_0)^{\frac{1}{b_0}} N^{\left(\frac{1}{b_0} - \frac{1}{b}\right)}}{(K)^{\frac{1}{b}}} \quad (32)$$

Substituting equation (32) into equation (29) yields

$$\frac{\sigma_{ls}}{\sigma_{0s}} = \frac{\sigma_f}{\sigma_{0f}} = \frac{(K_0)^{\frac{1}{b_0}} N^{\left(\frac{1}{b_0} - \frac{1}{b}\right)}}{(K)^{\frac{1}{b}}} \quad (33)$$

From equation (33) it is evident that  $b_0$  must equal to  $b$  because  $\sigma_{ls}$  and  $\sigma_{0s}$  are independent of number of cycles  $N$ , i.e.,

$$b = b_0 \quad ; \quad K = \frac{K_0}{\left(\frac{\sigma_{ls}}{\sigma_{0s}}\right)^{b_0}} \quad (34)$$

From the above equations the constants  $b$  and  $K$  can be calculated analytically if fatigue strength curve of unidirectional laminate is given, i.e., the S-N curve of general laminates can be determined by a S-N curve of unidirectional laminate.

Constant  $B$ , which characterizes the coupled effects of matrix cracking and delamination on laminate stiffness degradation, is more difficult to obtain than constants  $b$  and  $K$ . O'Brien [2], using elastic Hooke's law, proposed an analytical equation to calculate laminate compliance degradation due to delamination from a matrix crack (see

Appendix B), i.e.,

$$S = \frac{1}{E} = \frac{a}{l E_{lam}} \left( \frac{t E_{lam}}{t_{ld} E_{ld}} - 1 \right) + \frac{1}{E_{lam}} \quad (35)$$

where  $S$  and  $a/l$  are laminate compliance and the ratio of local delamination length to laminate length, respectively,  $E_{ld}$  and  $t_{ld}$  represent the modulus and thickness of delaminated region in the vicinity of the matrix crack, and  $E_{lam}$  and  $t$  represent modulus and thickness of the undelaminated region. Differentiating equation (35) gives

$$\frac{dS}{da} = \frac{1}{l E_{lam}} \left( \frac{t E_{lam}}{t_{ld} E_{ld}} - 1 \right) \quad (36)$$

In another formulation, according to assumption 2 and equation (12), the laminate compliance degradation can be expressed by

$$S = \frac{1}{E} = \frac{1}{E_{lam} (1 - C_d \frac{A}{A^*})} = \frac{1}{E_{lam} (1 - C_d \frac{a}{l})} \quad (37)$$

Making a power series expansion for equation (37) and taking only linear terms, it is easy to see that equation (37) will reduce to the same form as equation (35), which means that the assumption 2 is reasonable. Differentiating equation (37) in terms of delamination length  $a$ , and then comparing with equation (36), yields

$$\frac{1}{l E_{lam}} \left( \frac{t E_{lam}}{t_{ld} E_{ld}} - 1 \right) = \frac{C_d}{E_{lam} l (1 - C_d \frac{a}{l})^2} \quad (38)$$

Substituting equation (26) into equation (38) and noting that  $D_d = a/l$  yields

$$B = \frac{\log(K N \sigma_{max}^b)}{\log\left(\frac{1-C}{1-q}\right)} \quad (39)$$

where

$$C^2 = \frac{C_d}{\left(\frac{t E_{lam}}{t_{ld} E_{ld}} - 1\right)} \quad (40)$$

Constant B now can be calculated by Equation (39) if number of fatigue cycles N at onset of local delamination is given; this may be obtained by O'Brien's equation (see Appendix B),

$$m \log N = \frac{\sigma_{max}^2 t}{2 n E_{lam}} \left(\frac{t E_{lam}}{t_{ld} E_{ld}} - 1\right) - G_c \quad (41)$$

where  $G_c$  and  $m$  are material parameters and  $n$  is number of delaminated surface. Ref. [10] also provides various test curves for determining the values of  $G_c$  and  $m$ .

It must be emphasized that equation (38) is not valid for the case where matrix cracking is the dominate failure mode such as in cross-ply laminates because constant  $C_d$  will reach zero. For this case we have to obtain new equation to calculate constant B. Based on the assumption proposed by Beaumont [17], the crack density growth rate  $dD_m/dN$  for cross-ply laminates can be expressed as

$$\frac{dD_m}{dN} = A \left(\frac{\sigma_{max}^2}{D_m}\right)^C \quad (42)$$

where  $A$  and  $C$  are unknown constants. Integrating equation (42) and noting that  $D_m = 0$  when  $N=0$  gives

$$D_m = [(C+1) A N]^{\frac{1}{C+1}} \sigma_{max}^{\frac{2C}{C+1}} \quad (43)$$

Assuming that expression of S-N curve is given by

$$K N_f \sigma_{\max}^b = 1 \quad (44)$$

where  $N_f$  is fatigue life under maximum fatigue stress  $\sigma_{\max}$ .  $b$  and  $K$  are unknown constants. Rewriting equation (43) gives

$$\frac{(C+1) A}{D_m^{C+1}} N \sigma_{\max}^{2C} = 1 \quad (45)$$

Comparing equation (44) with equation (45) and noting that  $C_m D_m = D_f$  when  $N=N_f$  gives

$$C = \frac{b}{2} \quad ; \quad A = \frac{K}{\left(1 + \frac{b}{2}\right) C_m} \left(\frac{D_f}{C_m}\right)^{\left(1 + \frac{b}{2}\right)} \quad (46)$$

Substituting equation (17) into equation (46), then into equation (43) yields

$$D_m = \left[ K N \sigma_{\max}^b \right]^{\left(1 + \frac{b}{2}\right)^{-1}} \frac{(1-q)}{C_m} \quad (47)$$

Substituting equation (7) into equation (47) gives

$$\frac{E}{E_0} = 1 - \left[ K N \sigma_{\max}^b \right]^{\left(1 + \frac{b}{2}\right)^{-1}} (1-q) \quad (48)$$

Now the constant  $B$  for cross-ply laminate can be obtained by comparing equation (25) with equation (48), i.e.,

$$B = 1 + \frac{b}{2} \quad (49)$$

Equation (49) will be used to calculate constant  $B$  for the case of  $C_d \approx 0$ . Up to now, all laminate parameters  $B$ ,  $b$  and  $K$  can be determined analytically by the above equations for general composite laminates. The prescribed parameters are, except for static materials properties,  $b_0$  and  $K_0$  which are from the S-N relation of a unidirectional laminate,  $G_c$  and  $m$  which are from the delamination resistance curve (see Appendix B or [2,14]).

Finally, it must be stated that analytical determination of constant  $B$  depends on many material parameters and equations, which means that the value of constant  $B$  is sensitive to these material parameters and equations. Thus if it is possible and accurate results are required, it is better to determine constant  $B$  by using experimental methods, which can be performed by use of measured stiffness data and the form of equation (25).

## CHAPTER 4

# ONSET OF EDGE DELAMINATION AND MATRIX CRACKING

The theory of total strain energy release rate is used to predict the onset of both matrix cracking and delamination. A simple analytical equation for prediction of onset of matrix cracking and delamination for the general laminates is developed in this chapter. The onset of critical strain  $\epsilon_c$  should be prescribed by experiments but approximately, one can use first ply failure theory at static load for onset of matrix cracking and fracture mechanics analysis for onset of edge delamination.

### 4.1 STRAIN ENERGY RELEASE RATE DUE TO MATRIX CRACKS

To predict the onset of edge delamination and matrix cracking, a theory of strain energy release rate was used. Considering an elastic body containing a crack of area  $A$  that grows under a constant applied nominal strain  $\epsilon$ , the strain energy release rate  $G$  is given by [16]

$$G = -V \frac{\epsilon^2}{2} \frac{dE}{dA} \quad (50)$$

where  $V$  is the volume of the body and  $dE/dA$  is the rate of stiffness change as the crack extends. The fundamental assumption of this work is that all of the matrix cracks in the

volume  $V$  is treated as a single equivalent crack. The crack area  $A$  can be expressed by

$$A = \sum_{i=1}^m A_i = \sum_{i=1}^m K_{mi} L \frac{W}{\cos\alpha} t_i = V \sum_{i=1}^m \frac{K_{mi}}{\sin\theta} \frac{t_i}{t} \quad (51)$$

Where (see Fig.4.1)

$m$  = total numbers of cracked plies

$K_{mi}$  = number of cracks per unit length at  $i$ th-cracked ply

$t_i$  = thickness of  $i$ th-cracked plies

$t$  = laminate thickness

$V$  = laminate volume,  $V=W L t$

$\theta$  = fibre angle of cracked plies orientated to the direction of loading ( $\alpha + \theta = 90^\circ$ )

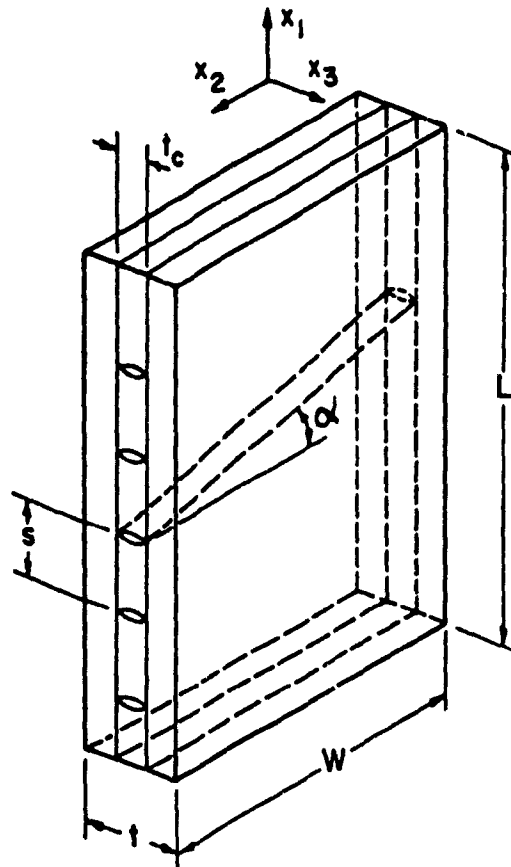


Fig. 4.1 Matrix cracking in a laminate [25]

Comparing equation (51) with equation (5) obtains

$$A = \frac{V}{t_c} D_m \quad (52)$$

Where  $t_c$  is thickness of first failure ply. Differentiating equation (52) yields

$$dA = \frac{V}{t_c} dD_m \quad (53)$$

The strain energy release rate due to matrix cracking,  $G_m$ , is obtained by substituting equation(53) into equation(50).

$$G_m = -V \frac{\epsilon^2}{2} \frac{dE}{dA} = -\frac{\epsilon^2 t_c}{2} \frac{dE}{dD_m} \quad (54)$$

Differentiating equation (7) and then substituting into equation (54) yields a simple expression of the strain energy release rate due to matrix cracking for the general laminates.

$$G_m = \frac{\epsilon^2 E_0 t_c C_m}{2} \quad (55)$$

## 4.2 STRAIN ENERGY RELEASE RATE DUE TO DELAMINATION

The expression of strain energy release rate due to edge delamination  $G_d$  can be obtained by differentiating equation (12) and then substituting the result into equation (50)

$$G_d = \frac{\epsilon^2 t}{2} (E_0 - E^*) \quad (56)$$

Equation (56) was first proposed by O'Brien [6] and was suggested for predicting onset of edge delamination. O'Brien states that equation (56) is not valid for the situation where the matrix cracking is the dominate failure mode because  $E_0 - E^*$  will reach zero. In this research a new equation is proposed, based on the theory of total strain energy release rate.

### 4.3 TOTAL STRAIN ENERGY RELEASE RATE

The total strain energy release rate,  $G$ , should include the effect of both matrix cracks and delamination, defined as

$$G = G_m + G_d \quad (57)$$

Substituting equation (55) and equation (56) into equation (57) gives

$$G = \epsilon^2 \left[ \frac{E_0 C_{mg} t_c}{2} + \frac{t (E_0 - E^*)}{2} \right] \quad (58)$$

The critical value of strain energy release rate  $G_c$  for the onset of edge delamination or matrix cracking is obtained from the actual onset strain  $\epsilon_c$  which should be determined by fatigue test, but, approximately, can be calculated by use of first ply failure theory for matrix cracking and fracture mechanics method for edge delamination. The equation (58) is more general than equation (56) for predicting the onset of delamination. Clearly, if the effect of matrix cracking on onset of edge delamination can be neglected, the equation (58) will reduce to equation (56). Instead of using equation (58), Equation (55) would be used to predict the onset of matrix cracking due to fatigue loading because matrix cracking always occurs earlier than delamination.

## CHAPTER 5

### FATIGUE LIFE PREDICTION

Fatigue life prediction of composite materials has been the subject of many investigations during the past two decades. Since composite materials exhibit very complex failure processes, an analytical model for predicting fatigue life directly in terms of physical damage such as matrix cracking and delamination for general composite laminates has not been found. The proposed approach in this chapter provides four choices for predicting fatigue life and for assessing fail-safety in structures made of composite laminates. These are: residual modulus criterion, matrix cracking criterion, delamination size criterion, and fatigue strength criterion.

#### 5.1 FATIGUE LIFE PREDICTION IN TERMS OF MATRIX CRACK DENSITY

Substituting equation (5) into equation (27) gives

$$N = \frac{(C_m \sum_{i=1}^m \frac{t_i^2 K_{mi}}{t \sin \theta_i})^B}{K \sigma_{\max}^b (1-q)^B} \quad (59)$$

Equation (59) can be used to predict fatigue life for general laminate if the allowable crack density  $K_m$  at each ply in the laminate is prescribed. All constants can be calculate by the equations derived in Chapter 3.

## 5.2 FATIGUE LIFE PREDICTION IN TERMS OF DELAMINATION

Fatigue failure life in terms of delamination area may be predicted by substituting allowable normalized delamination area  $D_d = A^0 / A^*$  into equation (26), that is,

$$N = \frac{(C_d \frac{A^0}{A^*})^B}{K \sigma_{\max}^b (1-q)^B} \quad (60)$$

It must be emphasized that  $C_d$  is a test constant and should be determined by fatigue tests. However, approximately,  $C_d$  can be obtained analytically by equation (13) if delamination is the dominant failure mode.

## 5.3 FATIGUE LIFE PREDICTION IN TERMS OF RESIDUAL STIFFNESS

Fatigue life in terms of residual stiffness can be calculated by use of equation (25). Rewriting equation (25) gives

$$N = \frac{(1 - \frac{E}{E_0})^B}{K \sigma_{\max}^b (1-q)^B} \quad (61)$$

Equation (61) is used to predict fatigue life for general laminates if the allowable residual stiffness in the laminate is prescribed. Clearly, if allowable residual stiffness  $E$  is equal to laminate failure stiffness  $E_f$ , then equation (61) will reduce to equation (22), i.e., reduced to the form of S-N curve.

#### **5.4 FATIGUE LIFE PREDICTION IN TERMS OF FATIGUE STRENGTH CURVE**

Fatigue life prediction in terms of applied stress is performed by using the S-N curve of a laminate, i.e., by using equation (22). The constants of S-N curve for a general laminate can be calculated by use of the relevant S-N curve of a unidirectional laminate (equation (34)). This is a traditional fatigue life analysis method but the direct relation of physical damage to fatigue failure life is not clear.

The meaning of all constants and variables in the equations of this chapter are same as those in Chapter 3. It is easy to see that all equations for prediction of fatigue life are other forms of equations in Chapter 3. The validity of these equations depends upon the credibility of equations in Chapter 3. Next chapter will provide four examples to illustrate and verify the proposed equations in Chapter 3.

## CHAPTER 6

### EXAMPLES

In this chapter,  $[0/90]_s$ ,  $[\pm 45/0/90]_s$ ,  $[0/\pm 45]_s$  glass/epoxy and  $\{0/90/\pm 45\}_s$  T300/5208 graphite/epoxy laminates under tension-tension fatigue loading ( $R=0.1$ ) were used to illustrate and verify the proposed approach. Figure 6.1 shows description of the problem, and static material properties are listed in Table 1. Experimental data was taken from [4, 16, 19, 20, 21]. Due to fact that an S-N relation for unidirectional laminates was not available, the best fit method and forms of equation (25) and equation (34) was applied to the measured stiffness loss data of a  $[0/90]_s$  glass/epoxy laminate and S-N curve of a  $[0/90/\pm 45]_s$  T300/5208 graphite/epoxy laminate to obtain constants of the unidirectional S-N curve ( $b_0$  and  $K_0$ ), and then calculations were performed for other laminates using these constants as prescribed parameters.

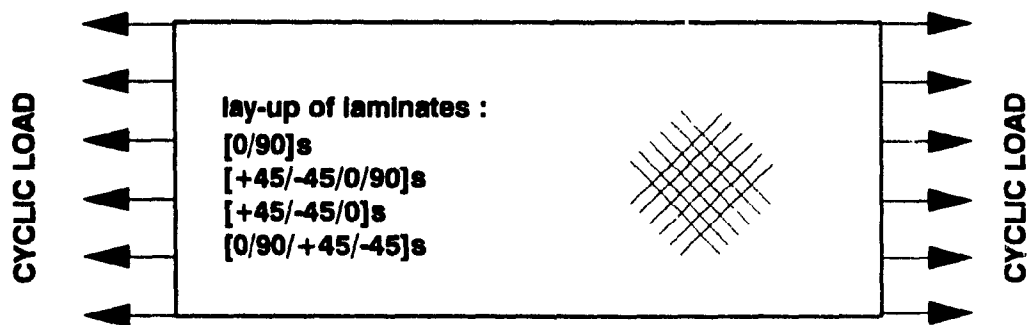


Fig. 6.1 description of the problem

**Table 1. Material properties of three E-glass/epoxy and one T300/5208 laminates**

laminates	$E_x$	$E_y$	$E_z$	$\nu_x$	$b_0$	$k_0$	$\sigma_{0s}$	$\sigma_{ls}$
$[\pm 45/0/90]_s$	43.7	16.0	6.3	0.28	7.0	1.0E-25	1060	330
$[0/90]_s$	41.7	13.0	3.4	0.3	7.0	1.0E-25	1060	520
$[0/\pm 45]_s$	41.7	13.0	3.4	0.3	7.0	1.0E-25	1060	400
$[0/90/\pm 45]_s$	181	10.3	7.17	0.28	17.3	2.38E-50	1500	540

The units of moduli and stress in Table 1 are GPa and MPa, respectively. The laminate static strength  $\sigma_{ls}$  is calculated by last-ply failure theory. Applied tension-tension maximum fatigue stress  $\sigma_{\max} = 160$ ,  $\sigma_{\max} = 207$ ,  $\sigma_{\max} = 175$  and  $\sigma_{\max} = 335$  have been used for the  $[\pm 45/0/90]_s$ ,  $[0/90]_s$ ,  $[0/\pm 45]_s$  and  $[0/90/\pm 45]_s$  specimens, respectively.

## 6.1 CROSS-PLY E-GLASS/EPOXY LAMINATE

Substitution of given material properties into equation(34) gives the following values for constants b and K.

$$b=7 ; K= 1.28E-23$$

Using laminate plate theory and equation (13) gives  $C_d \approx 0$ , which means that the effect of delamination on stiffness degradation is very small and the dominant mode of failure is matrix cracking. Equation (39) is no longer valid for this case, thus equation (49) is used to calculate constant B, i.e.,

$$B = 1 + b/2 = 4.5$$

Using equation (16) and noting that safety factor  $F_s$  is taken as 1.25 (see [4]) gives

$$q = \sigma_{\max} / \sigma_u = \sigma_{\max} F_s / \sigma_{ls} = 207 \times 1.25 / 520 = 0.5$$

Using equation (8) gives the value of constant  $C_m$

$$C_m = 0.45$$

Substituting the values of  $B$ ,  $b$ ,  $K$ ,  $q$ , and  $C_m$  into equation (25) and equation (27) gives

$$\frac{E}{E_0} = 1 - 0.5 ( 1.28 \times 10^{-23} N \sigma_{\max}^7 )^{0.22} \quad (62)$$

and

$$D_m = 1.1 ( 1.28 \times 10^{-23} N \sigma_{\max}^7 )^{0.22} \quad (63)$$

Figure 6.2 represents the comparisons of equations (62) and (63) with test data [19].

## 6.2 $[\pm 45/0/90]_S$ E-GLASS/EPOXY LAMINATE

Substitution of given material properties into equation (34) gives the following values for constants  $b$  and  $K$ .

$$b=7 ; K= 3.53E-22$$

Based on the first ply failure theory and Appendix B, using equation (13) in conjunction with laminate plate theory yields

$$t/t_{ld} = 1.33 ; E_{ld} = 27.11 \text{ GPa} ; C_d = 0.135$$

The number of cycles  $N$  at onset of local delamination due to matrix cracking is obtained by using equation (B11) in Appendix B, that is,

$$N = 6850 \text{ cycles}$$

Using equation (8) and equation (16) gives

$$C_m = 0.44 ; q = \sigma_{\max} / \sigma_u = \sigma_{\max} F_S / \sigma_{ls} = 0.61$$

Substituting above constants into equation (41) yields

$$B = 9.82$$

Substituting all results into equation (25) and equation (27) gives

$$\frac{E}{E_0} = 1 - 0.39 ( 3.53 \times 10^{-22} N \sigma_{\max}^7 )^{0.1} \quad (64)$$

$$D_m = 0.89 ( 3.53 \times 10^{-22} N \sigma_{\max}^7 )^{0.1} \quad (65)$$

Figure 6.3 represents the comparisons of equations (64) and (65) with experimental data [16].

### 6.3 $[0/\pm 45]_s$ E-GLASS/EPOXY LAMINATE

Analogous to calculations in section 6.2, it is easy to obtain following constants

$$b=7 ; K= 9.18E-23 ; B = 3.4 ; q =0.55$$

substituting the values of B, b, and K into equation (25) yields

$$\frac{E}{E_0} = 1 - 0.45 ( 9.18 \times 10^{-24} N \sigma_{\max}^7 )^{0.294} \quad (66)$$

Figure 6.4 represents the comparison of equation (66) with experimental data [19]. Matrix cracking damage  $D_m$  is not calculated because the test data is not available.

### 6.4 $[0/90/\pm 45]_s$ T300/5208 LAMINATE

Similar to calculations in sections 6.2 and 6.3, the following constants are

obtained

$$b=17.33 ; K= 1.16E-50 ; B = 6 ; q = 0.776 ; C_m = 0.47$$

Substituting the above results into equation (25) and equation (27) gives

$$\frac{E}{E_0} = 1 - 0.224 ( 1.16 \times 10^{-50} N \sigma_{\max}^{17.3} )^{0.17} \quad (67)$$

$$D_m = 0.477 ( 1.16 \times 10^{-50} N \sigma_{\max}^{17.3} )^{0.17} \quad (68)$$

Figure 6.5 represents the comparisons of equations (67) and (68) with experimental data [4, 21].

## 6.5 FATIGUE STRENGTH CURVES

The fatigue strength (S-N curve) for the above laminates can be represented by

$$K N \sigma_{\max}^b = 1 \quad (69)$$

Constants  $b$  and  $K$  in equation (69) can be calculated by use of the relevant S-N curve of a unidirectional laminate, i.e., equation (34). The figure 6.6 shows the fatigue strength versus fatigue cycles for the above laminates.

## 6.6 SUMMARY

From figures 6.2 to 6.5 it is seen that analytical results are in good agreement with experimental data for the above examples. However, due to experimental data unavailable for the unidirectional laminates and very complex fatigue behavior of the laminates, more experiments should be performed to verify or modify the models developed by this research.

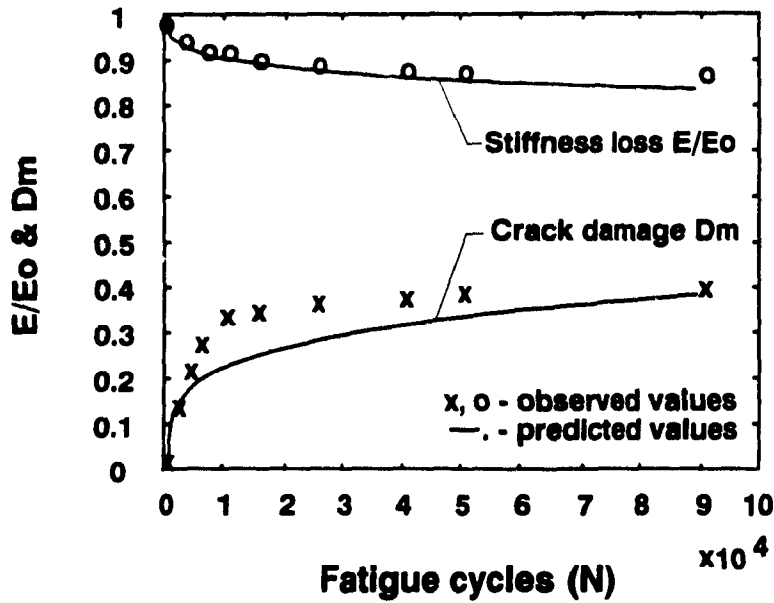


Fig. 6.2 Variation of longitudinal stiffness and crack damage versus fatigue cycles for a  $[0/90]_s$  E-glass/epoxy laminate.

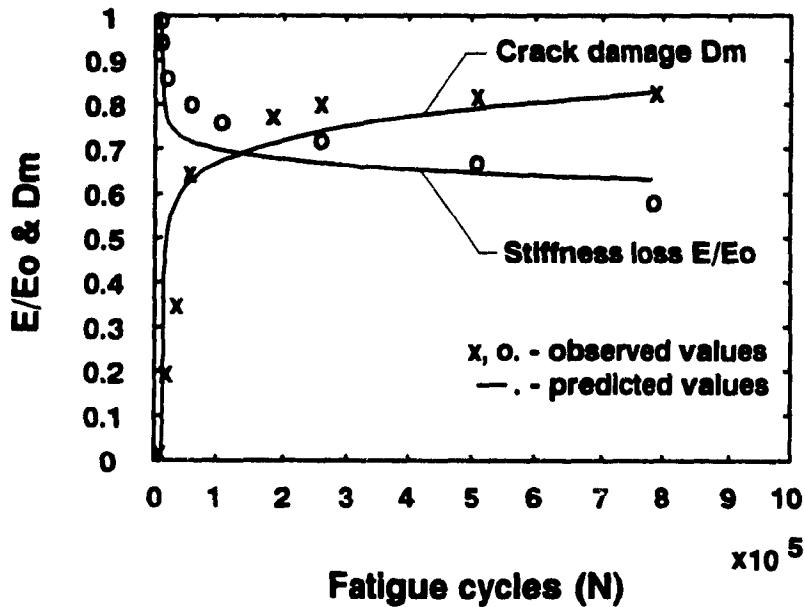


Fig. 6.3 Variation of longitudinal stiffness and crack damage versus fatigue cycles for a  $[+45/-45/0/90]_s$  E-glass/epoxy laminate.

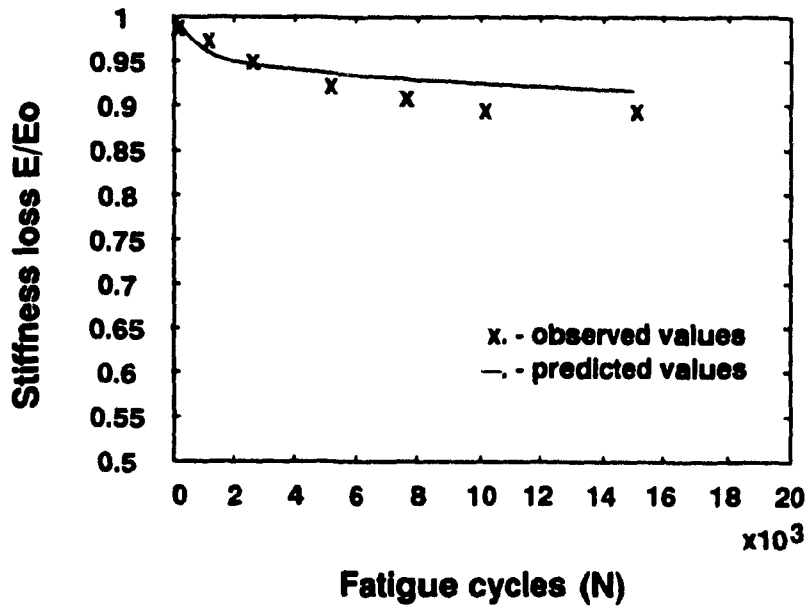


Fig. 6.4 Variation of longitudinal stiffness versus fatigue cycles for a  $[0/+45/-45]_s$  E-glass/epoxy laminate.

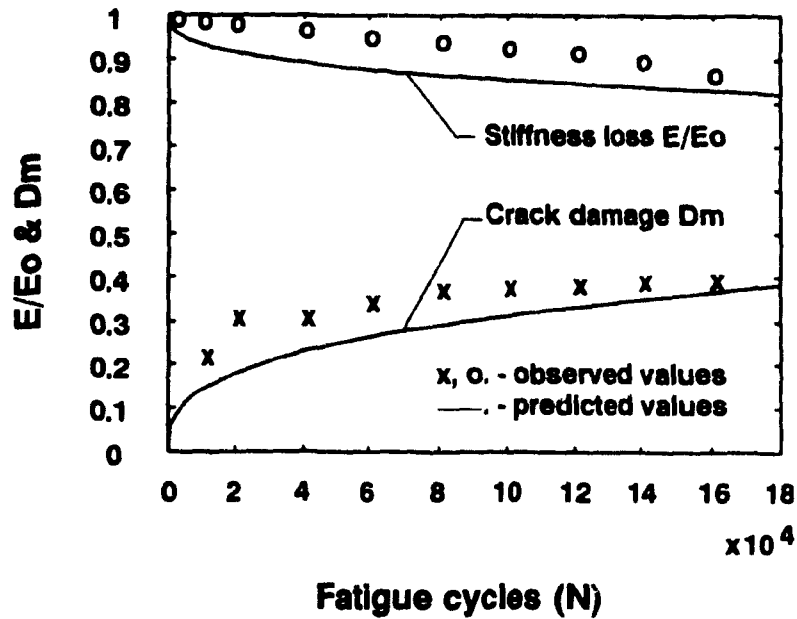


Fig. 6.5 Variation of longitudinal stiffness and crack damage versus fatigue cycles for a  $[0/90/+45/-45]_s$  T300/5208 laminate.

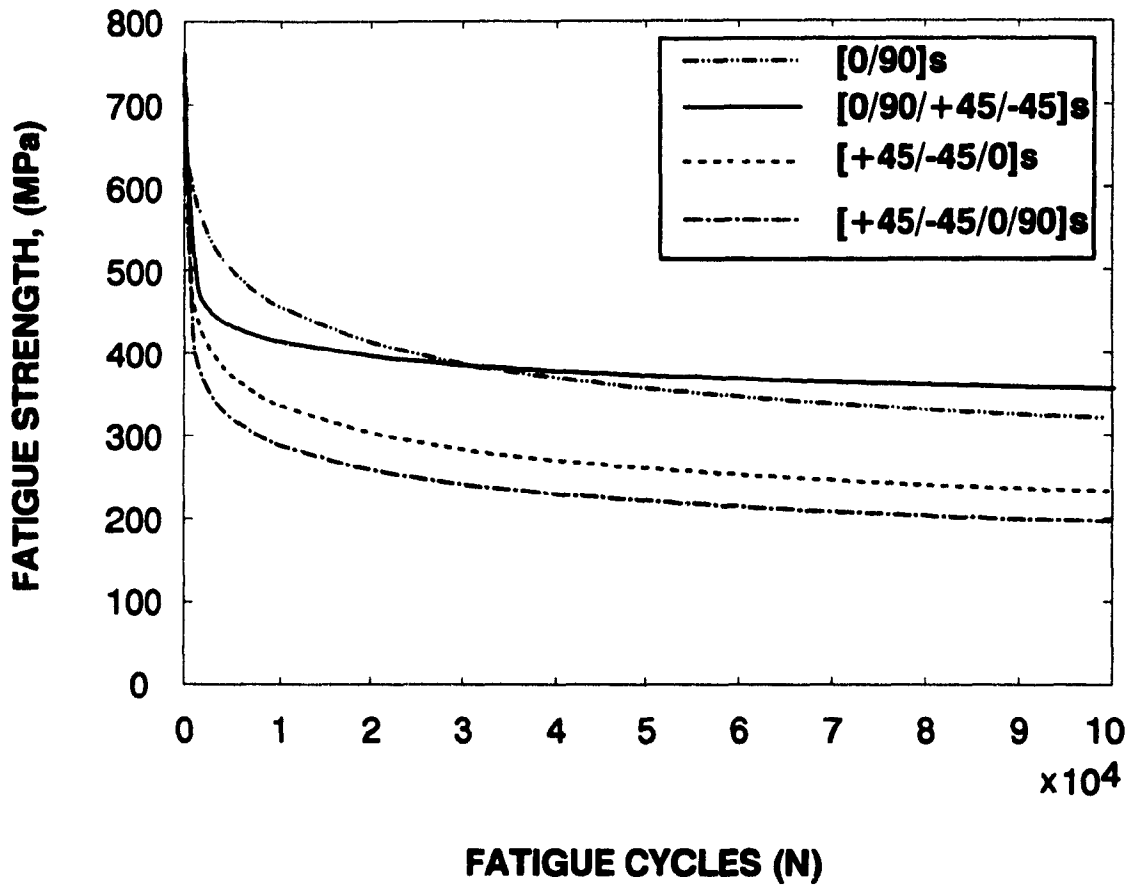


Fig. 6.6 S-N curves for [0/90]s, [+45/-45/0/90]s, [0/+45/-45]s glass/epoxy and [0/90/+45/-45]s T300/5208 graphite/epoxy laminates

## CHAPTER 7

# NOTCHED LAMINATES UNDER CYCLIC LOADING

The fatigue response of unnotched composite laminates to cyclic loading has been studied in detail in previous chapters. Another particularly important aspect of the fatigue of composite materials is behavior of laminates with geometric discontinuities such as holes, joints, ply terminations, and/or inherent defects. The performance of notched laminates under fatigue loading is controlled by the stress fields and material performance in the neighbourhood of stress concentrators such as cutouts of various types, the most common being a joint or access hole. While the initiation of damage in these regions has been studied in some detail [22,23], growth of damage from such geometric discontinuities under cyclic loading has received relatively little systematic attention, and modelling of such growth has been limited to particular laminates. At the present time, the complex damage growth process has not been rigorously investigated or described, fatigue strength and fatigue failure life can not be reliably predicted, and, consequently, new and existing material systems can not be exploited safely, efficiently, and completely.

In metals, the problem of stress concentration resulting from various notches is well defined by the many stress concentration factors which influence the behavior under cyclic stress, and crack propagation is easily related to specimen data through the use of fracture mechanics. In notched composite laminates, however, the damage modes and growth around notches are seen to be quite different. Multiple cracks coupled with

delamination are often observed in the region around notches, and combined stresses are produced and vary widely around the notch during the fatigue life of a laminate. When damage occurs, changes of moduli around the notch result in changes of magnitude and redistribution of stresses. The subsequent stress analysis becomes very difficult. The stress redistribution after fatigue damage has made it difficult to predict the fatigue strength of notched laminate using the fatigue strength of the unnotched specimens.

This chapter addresses the specific subject of fatigue response of a laminate with a central hole subjected to tension-tension cyclic load. Due to changing of materials properties at failed regions, the closed form solution of stresses around the hole is not valid. The finite element technique is used for stress analysis in this research and the stress analysis was carried out by using well-known NASTRAN Software. Equation (28) is used to model changes of residual moduli as function of fatigue load and number of cycles. This new analysis approach will be compared with experimental results.

## **7.1 OVERVIEW OF FINITE ELEMENT METHOD FOR COMPOSITE LAMINATES**

The following overview of the theory in NASTRAN's capability for the analysis of laminated composites is based on classical lamination theory which incorporates the following assumptions:

1. The laminate consists of perfectly bonded plies.
2. displacements are continuous across laminate boundaries.
3. Each of the lamina is in a state of plane stress.

The material properties of structures modeled with plate and shell elements including the isoparametric quadrilateral element and the triangular element are reflected in the following matrix relation between force and strains.

$$\begin{Bmatrix} f \\ m \\ q \end{Bmatrix} = \begin{bmatrix} TG_1 & T^2G_4 & 0 \\ T^2G_4 & IG_2 & 0 \\ 0 & 0 & T_sG_3 \end{bmatrix} \begin{Bmatrix} \epsilon_m - \epsilon_m^t \\ X - X^t \\ \gamma \end{Bmatrix} \quad (70)$$

where

$$\{ f \} = \begin{Bmatrix} f_x \\ f_y \\ f_{xy} \end{Bmatrix}, \quad \text{membrane forces per unit length} \quad (71)$$

$$\{ m \} = \begin{Bmatrix} m_x \\ m_y \\ m_{xy} \end{Bmatrix}, \quad \text{bending moments per unit length} \quad (72)$$

$$\{ q \} = \begin{Bmatrix} q_x \\ q_y \end{Bmatrix}, \quad \text{transverse shear force per unit length} \quad (73)$$

$$\{ \epsilon_m \} = \begin{Bmatrix} \epsilon_x \\ \epsilon_y \\ \epsilon_{xy} \end{Bmatrix}, \quad \text{membrane strains} \quad (74)$$

$$\{ X \} = \begin{Bmatrix} x_x \\ x_y \\ x_{xy} \end{Bmatrix}, \quad \text{curvatures} \quad (75)$$

$$\{ \gamma \} = \begin{Bmatrix} \gamma_x \\ \gamma_y \end{Bmatrix}, \quad \text{transverse shear strain} \quad (76)$$

The quantity  $[G_3]$  is a  $2 \times 2$  matrix of elastic coefficients for transverse shear and

$T_e$  is the effective thickness for transverse shear. The vectors  $\{\varepsilon_m\}$  and  $\{X\}$  are thermal strains and curvatures respectively (note that thermal effects are not considered in this research). The terms  $T$  and  $I$  are the membrane thickness and bending inertia per unit width, respectively. The terms  $G_1$ ,  $G_2$ , and  $G_4$  are defined by the following integrals:

$$\begin{aligned} G_1 &= \frac{1}{T} \int [G_e] dz \\ G_2 &= \frac{1}{T} \int z^2 [G_e] dz \\ G_4 &= \frac{1}{T^2} \int -z [G_e] dz \end{aligned} \quad (77)$$

The limits on the integration are from the bottom surface to the top surface of the laminated composite. The matrix of material moduli,  $[G_m]$ , has the following form for orthotropic materials:

$$[G_m] = \begin{bmatrix} \frac{E_1}{1-\nu_1\nu_2} & \frac{\nu_1 E_2}{1-\nu_1\nu_2} & 0 \\ \frac{\nu_2 E_1}{1-\nu_1\nu_2} & \frac{E_2}{1-\nu_1\nu_2} & 0 \\ 0 & 0 & G_{12} \end{bmatrix} \quad (78)$$

For linearly elastic materials,  $\nu_1 E_2 = \nu_2 E_1$  in order to satisfy the requirement that the matrix of elastic moduli is symmetric. In general, the analysis may supply properties with respect to a particular orientation which does not necessarily correspond to the principal materials axes. In this case, the analysis must also supply the value of the angle,  $\theta$ , that orients the element axis relative to side of the element. The materials stiffness matrix is then transformed into the element stiffness matrix through the relation

$$[G_e] = [v]^T [G_m] [v] \quad (79)$$

where

$$[v] = \begin{bmatrix} \cos^2\theta & \sin^2\theta & \cos\theta\sin\theta \\ \sin^2\theta & \cos^2\theta & -\cos\theta\sin\theta \\ -2\cos\theta\sin\theta & 2\cos\theta\sin\theta & \cos^2\theta\sin^2\theta \end{bmatrix} \quad (80)$$

Finite element models for structures made of composite materials require the evaluation of the matrix of elastic moduli for each plate element of the model. The characteristics of composite materials are totally contained in these matrices. Once these matrices of elastic moduli are calculated, the analysis will proceed in a standard manner of finite element technique. The calculation of stresses and strains in individual ply can be performed by using the lamination theory of transformation.

## 7.2 CALCULATION OF RESIDUAL MODULI UNDER BI-DIRECTIONAL CYCLIC LOADING

The main difference in the finite element model between static load and cyclic load is the degradation of elastic moduli. The degradation of elastic moduli under cyclic loading in a damaged region is a function of both stress level and number of cycles. An analytic model relating residual moduli to fatigue stress and number of cycles has already been developed in Chapter 3. Equation (28) and equation (29) will be utilized to represent this relation. The following assumptions have to be made :

1. When an element is subjected to bi-directional fatigue load, linear superposition of the effect of these two load components on change of elastic moduli is performed.
2. The effect of shear load on change of elastic moduli is neglected. This is reasonable because the shear stresses around the hole are much smaller than tension stresses.

Based on the above assumptions, the reduction of elastic moduli under bi-directional

plane cyclic loading can be modeled as follows

$$\begin{aligned}
 E_1 &= E_1^0 - (\Delta E_1^1 + \Delta E_1^2) \\
 E_2 &= E_2^0 - (\Delta E_2^1 + \Delta E_2^2) \\
 \nu_1 &= \nu_1^0 - (\Delta \nu_1^1 + \Delta \nu_1^2) \\
 G_{12} &= G_{12}^0 - (\Delta G_{12}^1 + \Delta G_{12}^2)
 \end{aligned} \tag{81}$$

where the reduction of elastic moduli under cyclic loading  $\sigma_1$  can be obtained by using equation (28) and equation (29), i.e.,

$$\begin{aligned}
 \Delta E_1^1 &= -\frac{2(1-q)}{C_{m1}} (K_1 N \sigma_1^{b_1})^{\left(\frac{1}{B_1}\right)} [k_3 + k_7(\nu_{12}^0)^2 - k_{13}\nu_{12}^0] \\
 \Delta E_2^1 &= -\frac{2(1-q)}{C_{m1}} (K_1 N \sigma_1^{b_1})^{\left(\frac{1}{B_1}\right)} [k_7 + k_3(\nu_{21}^0)^2 - k_{13}\nu_{21}^0] \\
 \Delta \nu_1^1 &= -\frac{(1-q)}{C_{m1}} (K_1 N \sigma_1^{b_1})^{\left(\frac{1}{B_1}\right)} \left[ \frac{1 - \nu_{12}^0 \nu_{21}^0}{E_2^0} \right] (k_{13} - 2k_7 \nu_{12}^0) \\
 \Delta G_{12}^1 &= -\frac{2(1-q)}{C_{m1}} (K_1 N \sigma_1^{b_1})^{\left(\frac{1}{B_1}\right)} k_{11}
 \end{aligned} \tag{82}$$

and the reduction of elastic moduli under cyclic loading  $\sigma_2$  gives

$$\begin{aligned}
 \Delta E_2^2 &= -\frac{2(1-q)}{C_{m2}} (K_2 N \sigma_2^{b_2})^{\left(\frac{1}{B_2}\right)} [k_3 + k_7(\nu_{21}^0)^2 - k_{13}\nu_{21}^0] \\
 \Delta E_1^2 &= -\frac{2(1-q)}{C_{m2}} (K_2 N \sigma_2^{b_2})^{\left(\frac{1}{B_2}\right)} [k_7 + k_3(\nu_{12}^0)^2 - k_{13}\nu_{12}^0] \\
 \Delta \nu_1^2 &= -\frac{(1-q)}{C_{m2}} (K_2 N \sigma_2^{b_2})^{\left(\frac{1}{B_2}\right)} \left[ \frac{1 - \nu_{12}^0 \nu_{21}^0}{E_2^0} \right] (k_{13} - 2k_7 \nu_{21}^0) \\
 \Delta G_{12}^2 &= -\frac{2(1-q)}{C_{m2}} (K_2 N \sigma_2^{b_2})^{\left(\frac{1}{B_2}\right)} k_{11}
 \end{aligned} \tag{83}$$

The determination of constants of the above equations can be performed by using relevant

equations in Chapter 3.

### **7.3 FATIGUE ANALYSIS BY USING THE FINITE ELEMENT TECHNIQUE**

It is very difficult to model fatigue damage growth and to predict fatigue life by using finite element techniques due to lack of analytical models for predicting elastic moduli degradation. Fortunately, a new approach for calculating residual moduli as a function of stress level and number of cycles for general composite laminates has been developed by the present research and is extended to the analysis of notched laminates in conjunction with finite element techniques. The modulus degradation criterion is chosen to define failure of the elements around the hole because modulus reduction may include damage in both delamination and matrix cracking modes. The value of critical residual modulus can be obtained from an unnotched specimen by many methods described in previous chapters including fatigue test data, strain failure criterion, delamination law, and so on. In general, if it is possible and accurate results are required, fatigue test data should be used for determining the value of critical residual modulus, but approximately, delamination law or strain failure criterion can be used to calculate critical residual modulus analytically. Figure 7.1 represents the flow chart of this analytical process.

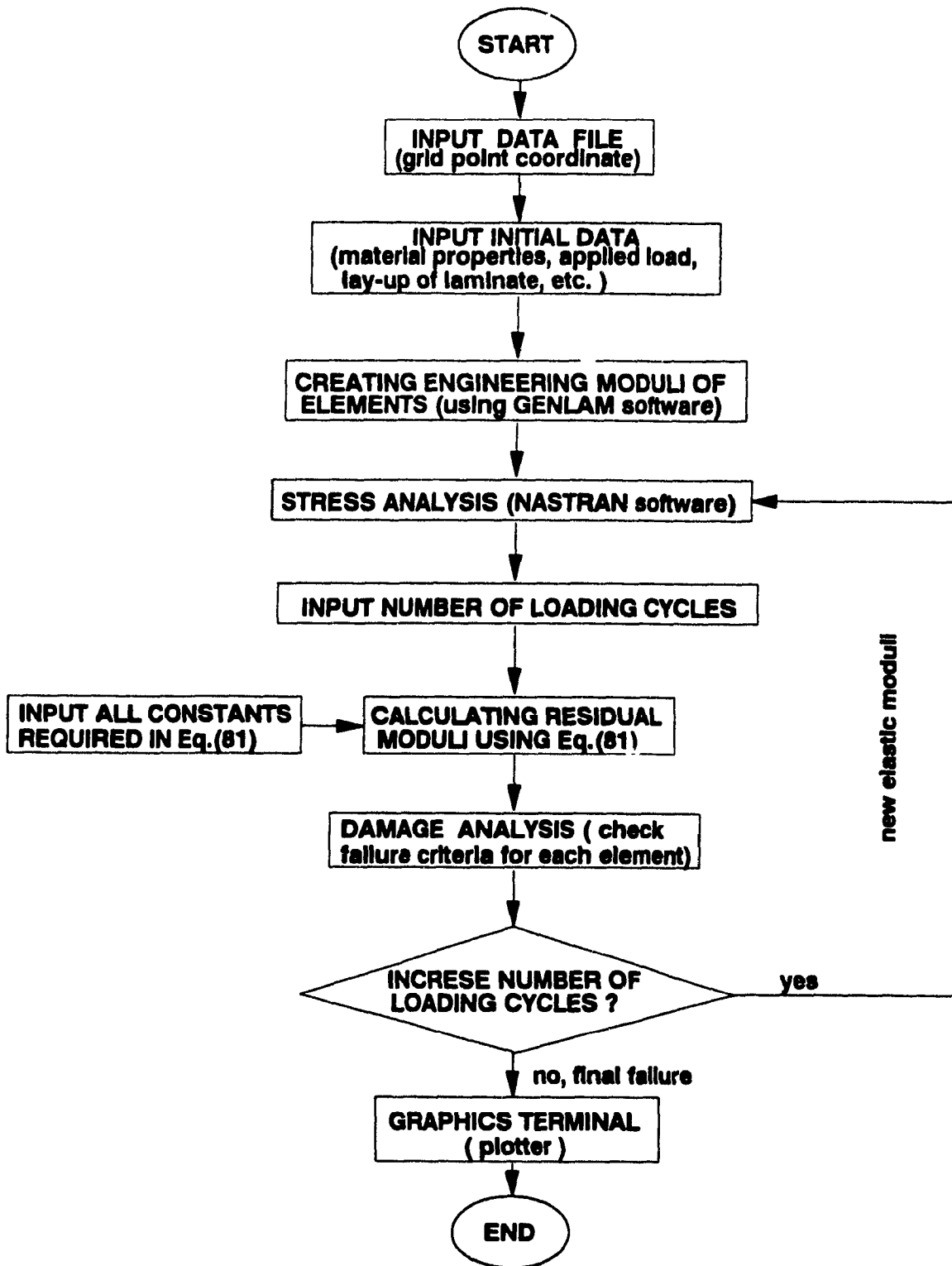


Fig. 7.1 Flow chart of fatigue analysis process in notched laminated plate using the finite element method.

## 7.4 EXAMPLE

To illustrate and verify the fatigue failure process by using finite elements, consider a quasi-isotropic plate containing a circular hole located at the center of the plate as shown in Figure 7.2. The specimen is a  $[0/90/\pm 45]_s$  T300/5208 graphite/epoxy laminate. Width  $W$  and length  $L$  of the specimen are 38 mm and 90 mm, and diameter  $d$  and thickness  $t$  are 9 mm and 2 mm, respectively. A tension-tension fatigue load with maximum stress 218.5 MPa is applied at two ends of the specimen, and the ratio of maximum stress to minimum stress  $R$  is equal to 0.1. Figure 7.3 represents the finite element model of this problem. Dimensions of the specimen used in the calculation are taken from Ref.[24]. The material properties are listed in Table 2.

Table 2 Material properties for a  $[0/90/\pm 45]_s$  T300/5208 specimen

$E_1^0$ (GPa)	$E_2^0$ (GPa)	$G_{12}^0$ (GPa)	$\nu_{12}^0$ (--)	$\sigma_{0s}$ (MPa)	$\sigma_{1s}$ (MPa)	$m$ (--)	$G_c$ (J/m <sup>2</sup> )	$b_0$ (--)	$K_0$ (--)
69.68	69.68	26.88	0.3	1500	540	-23	200	17.33	2.4E-58

In Table 2 the laminate engineering moduli  $E_1^0$ ,  $E_2^0$ ,  $G_{12}^0$  and  $\nu_{12}^0$  are calculated by using laminate plate theory (GENLAM software),  $\sigma_{0s}$ ,  $\sigma_{1s}$ ,  $b_0$  and  $K_0$  are taken from Table 6.1 in Chapter 6, and constants  $m$  and  $G_c$  are from Appendix B.

Analogous to the calculation process in Chapter 6, it is easy to obtain the following constants in equations (82) and (83)

For  $[0/90/\pm 45]_s$  lay-up, i.e., in the direction of  $\sigma_1$  :

$$B_1 = 6, \quad b_1 = 17.3, \quad K_1 = 1.16E-50, \quad C_{m1} = 0.47$$

For  $[90/0/\pm 45]_s$  lay-up, i.e., in the direction of  $\sigma_2$ :

$$B_2 = 8, \quad b_2 = 17.3, \quad K_2 = 1.16E-50, \quad C_{m2} = 0.47$$

Substituting all constants into equation (82) and equation (83), and then into equation (81) gives the expression for residual moduli of a  $[0/90/\pm 45]_s$  T300/5208 specimen under bi-directional fatigue load as

$$\begin{aligned} E_1 &= E_1^0 - (3.15 \times 10^{-16} N^{0.167} \sigma_1^{2.88} + 3.32 \times 10^{-14} N^{0.125} \sigma_2^{2.16}) \\ E_2 &= E_2^0 - (1.61 \times 10^{-18} N^{0.167} \sigma_1^{2.88} + 6.52 \times 10^{-12} N^{0.125} \sigma_2^{2.16}) \\ \nu_1 &= \nu_1^0 - (6.95 \times 10^{-19} N^{0.167} \sigma_1^{2.88} + 1.65 \times 10^{-14} N^{0.125} \sigma_2^{2.16}) \\ G_{12} &= G_{12}^0 - (6.21 \times 10^{-19} N^{0.167} \sigma_1^{2.88} + 1.28 \times 10^{-14} N^{0.125} \sigma_2^{2.16}) \end{aligned} \quad (84)$$

Critical residual stiffness has to be prescribed. Based on O'Brein's delamination theory, in this example the delamination law is utilized to calculate critical value of residual stiffness because of its simplicity. The accuracy of this choice is verified by test data. The residual stiffness when completely delaminated along 0 degree and 90 degree interface is defined as critical residual stiffness and is obtained by using equation (10)

$$E_1^f = E^* = 0.86 E_1^0 = 60 \text{ MPa}$$

where  $E_1^f$  is defined as the critical value of residual stiffness  $E_1$ . This result is evident from test data in figure 6.5 where  $E_1 / E_1^0$  approaches to 0.85 after a large number of cycles. During the calculation using the finite element method, the failure level for an element of the structure is defined as "when residual stiffness of an element is equal to its critical stiffness, the element is failed."

Figure 7.4 shows graphical representation of damage growth of a  $[0/90/\pm 45]_s$  T300/5208 graphite/epoxy laminated plate under fatigue loading. Figure 7.5 presents

radiographs of damage growth for the same specimen under fatigue loading. From Figure 7.4 the predicted life is about  $1 \times 10^6$  cycles which agrees with experimental data [24].

## 7.5 SUMMARY

From the above theoretical analysis and example it can be seen that analytical results using finite element techniques approximately agree with experimental data for a  $[0/90/\pm 45]_s$  T300/5208 graphite/epoxy laminate under fatigue loading. As we know, the fatigue behavior of notched laminates is very complex and analytical methods in conjunction with finite element techniques to solve this kind of problem is just beginning. In general, it must take following factors into account:

1. Credible residual moduli reduction model after damage.
2. Appropriate failure criterion to check failure of elements.
3. Powerful computer software which includes finite element techniques.

In this research a simple example of a quasi-isotropic laminate was performed to illustrate and verify above analysis processes. The computer software developed in this research included GENLAM, NASTRAN software. Due to time limitations, iteration loops for computing damage extension are not performed automatically. In order to obtain detailed analysis of damage extension and fatigue failure life under fatigue loading, further work is needed to develop more powerful software, which should be able to integrate the whole computing process automatically (see flow chart in figure 7.1). In addition, more experiments should be performed to verify or modify the proposed models in this research.

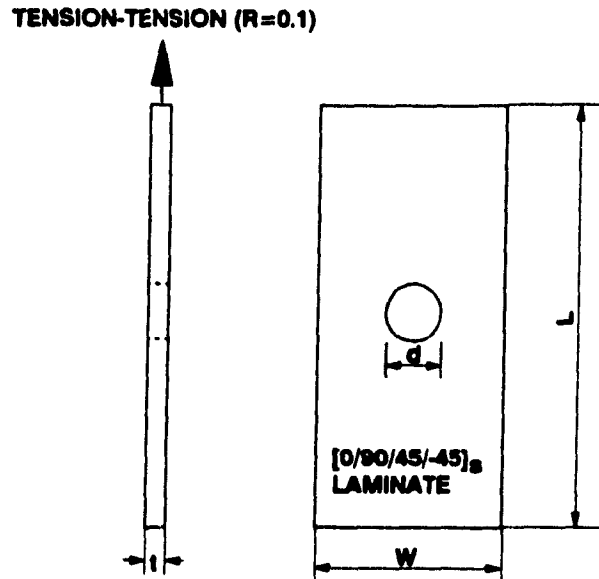


Fig. 7.2 - Description of the problem

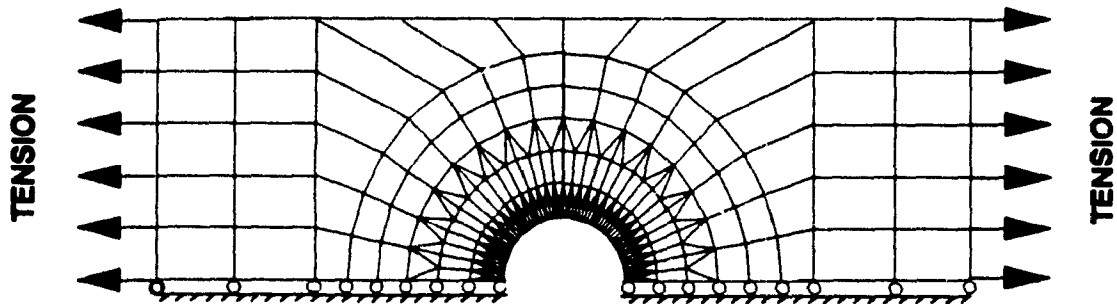
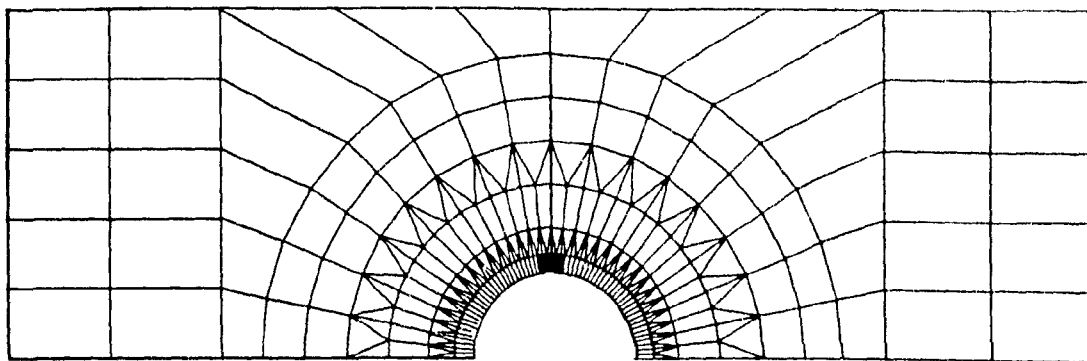
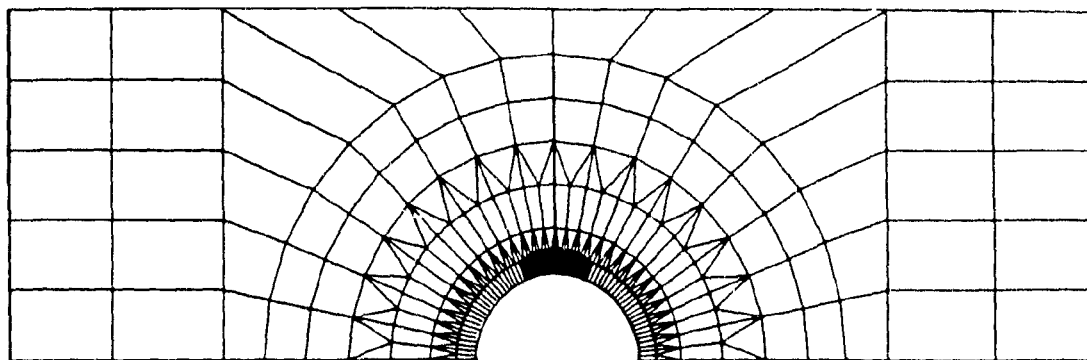
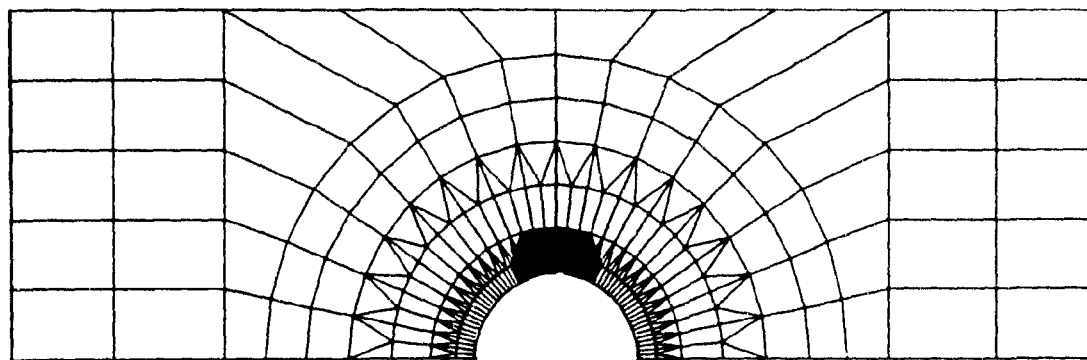
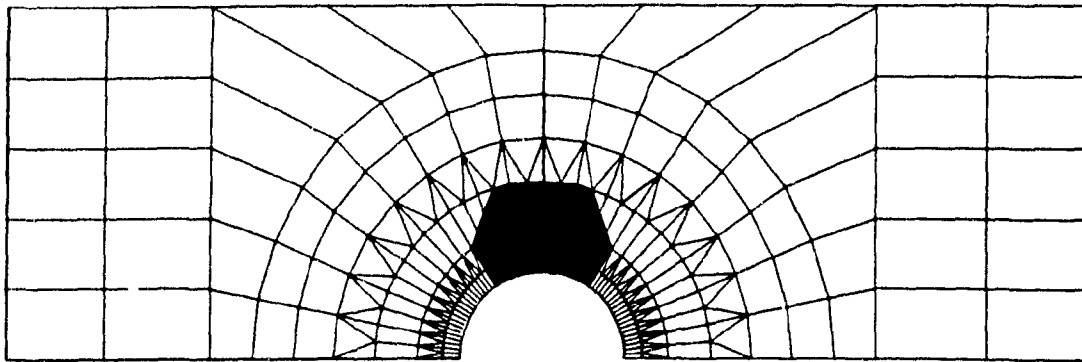


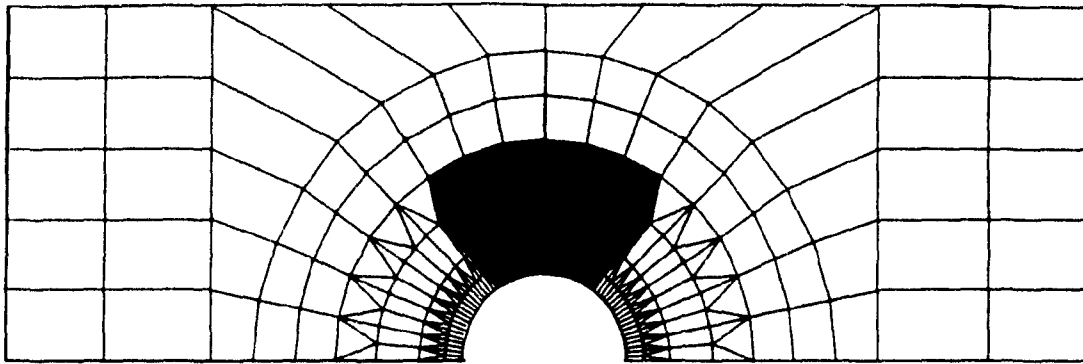
Fig. 7.3 - Finite element model of the problem

(a)  $N = 1$  CYCLES(b)  $N = 10$  CYCLES(c)  $N = 1000$  CYCLES

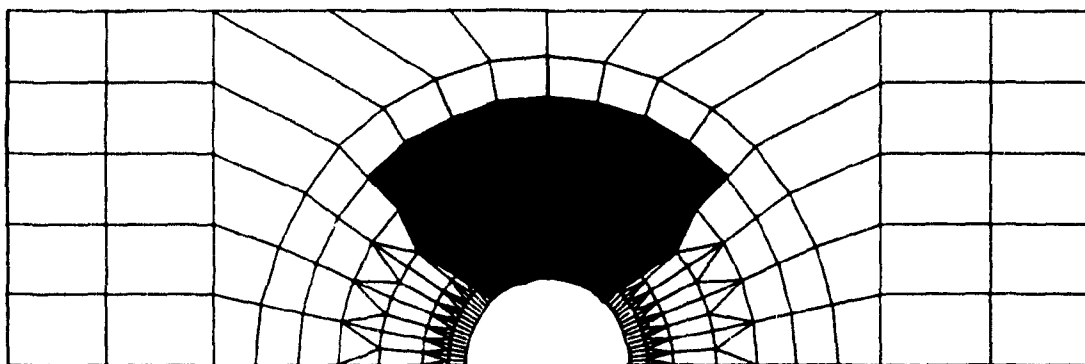
**Fig. 7.4** Graphical representation of damage growth of a  $[0/90/\pm 45]_s$  T300/5208 graphite/epoxy laminated plate under fatigue loading ( $\sigma_{\max} = 0.8 \sigma_{sk} = 218.5$  MPa,  $R = 0.1$ ).



(d)  $N = 10,000$  CYCLES



(e)  $N = 100,000$  CYCLES

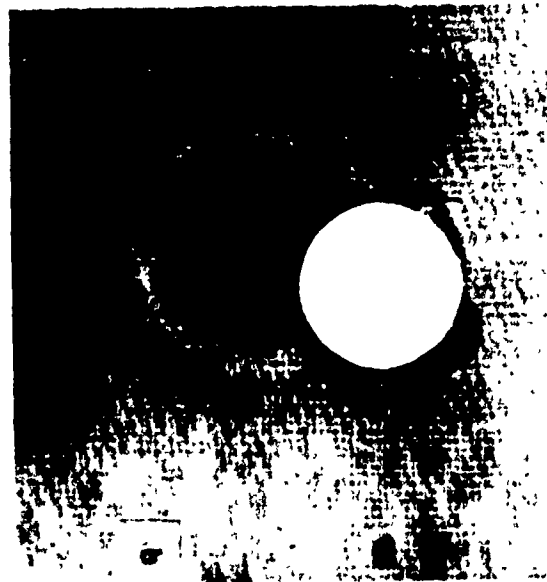


(f)  $N = 600,000$  CYCLES

Fig. 7.4 continued

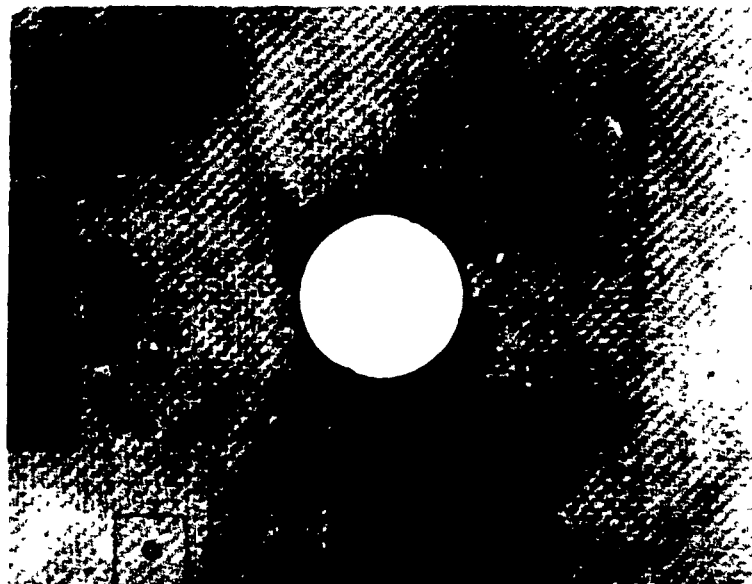


(a) N=10 cycles

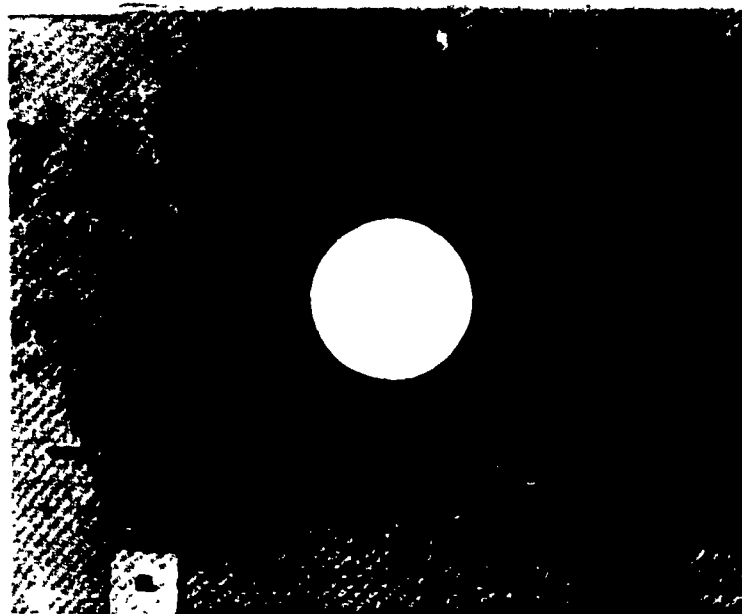


(b) N=1000 cycles

**Fig. 7.5** Radiographs of damage growth in a  $[0/90/\pm 45]_s$  T300/5208 graphite/epoxy laminated plate under fatigue loading ( $\sigma_{\max} = 0.8 \sigma_{ult} = 218.5$  MPa,  $R = 0.1$ ) [24]

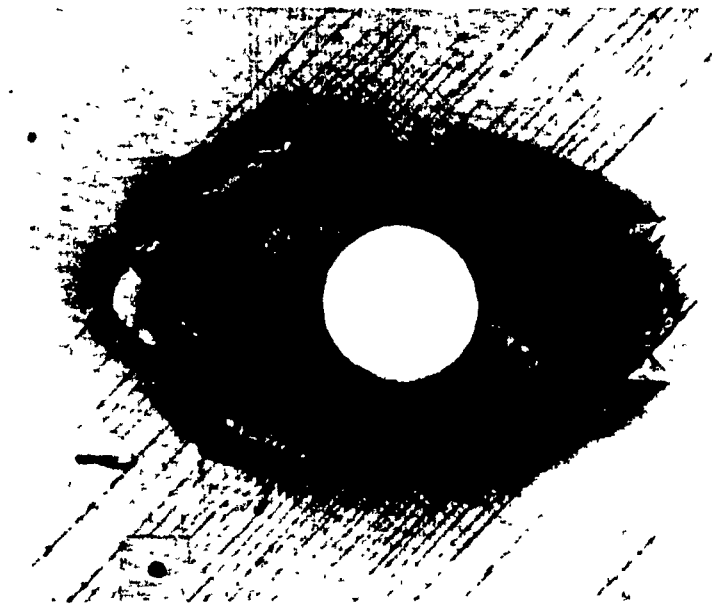


(c)  $N=1 \times 10^4$  cycles



(d)  $N=1 \times 10^5$  cycles

Fig. 7.5 continued



(e)  $N=6 \times 10^5$  cycles

Fig. 7.5 continued

## CHAPTER 8

### CONCLUSIONS AND RECOMMENDATIONS

The proposed analytical approach in this research is generic and allows for evaluation of the onset and growth of fatigue damage and prediction of fatigue failure life of laminated composites with arbitrary lay-up using a minimum of experimental measurements. The conclusions and recommendations are described as follows:

1. Based on the models by Talreja [3] and O'Brien [6], Residual Stiffness under fatigue load can be characterized approximately by a linear relation with matrix crack density and delamination area. Residual stiffness can be used as a global variable to predict matrix cracks, delamination area and fatigue failure life for the laminates under fatigue loading. Such an approach seems to have advantages over residual strength methods in that the residual stiffness can be measured nondestructively in service, whereas the measurement of the residual strength is destructive.
2. Global Damage variable growth rate  $dD/dN$  is proportional to some power of applied fatigue stress and inversely proportional to some power of current level of damage variable  $D$  itself (see equation(20)). Based on this assumption, the analytical model of modulus degradation in terms of fatigue stress and number of cycles was derived.
3. Strain energy release rates may be used to predict the onset of both matrix cracking and delamination. The onset of critical strain  $\epsilon_c$  should be prescribed by experiments but approximately, one can use first ply failure theory at static

load for onset of matrix cracking and fracture mechanics analysis for onset of edge delamination.

4. The proposed approach provided four choices for predicting tension-tension fatigue life and for assessing fail-safety for structures made of composite laminates, that is, residual modulus criterion, matrix cracking criterion, delamination area criterion and fatigue strength criterion.
5. The proposed approach enables prediction of fatigue behavior of general laminates using experimental data of a basic lay-up such as the unidirectional laminate. Three  $[0/90]_s$ ,  $[\pm 45/0/90]_s$ ,  $[0/\pm 45]_s$  E-glass/epoxy laminates and one  $[0/90/\pm 45]_s$  graphite/epoxy laminate under tension-tension fatigue loading were used to illustrate and verify the proposed approach and have good agreement with analytical results. For other layup configuration and different materials, more experiments should be performed to further verify the proposed model.
6. The fatigue behavior of notched laminates is very complex. The performance of notched laminates under fatigue loading is controlled by stress fields and materials performance in the neighbourhood of stress concentrators. The stress redistribution after fatigue damage has made it very difficult to perform stress analysis of notched laminate by using analytical or closed form methods. The moduli reduction model developed by this research and O'Brien's delamination law in conjunction with finite element techniques may be a useful method to model the fatigue process of notched laminates. In general, using this approach must take the following factors into account:
  - Credible residual moduli reduction model after damage.
  - Appropriate failure criterion to check failed elements.
  - Powerful computer software which includes finite element techniques.

In this research a simple example of a  $[0/90/\pm 45]_s$  T300/5208 graphite/epoxy laminate with a central hole under fatigue loading was performed to illustrate and verify the above analytical processes. The results, approximately, agree with experimental data. Due to time limitations, the iteration loop for computing damage extension is not performed automatically. In order to obtain detailed analysis of damage extension and fatigue failure life under fatigue loading, further work is needed to develop more powerful software, which should be able to integrate the entire computing process automatically (see flow chart in figure 7.1). In addition, more experiments should be performed to verify or modify the proposed models in this research.

## REFERENCES

1. Lessard, L.B. and Shokrieh, M.M. "Failure of laminated composite materials," International Conference on Engineering Applications of Mechanics, Tehran, Iran, June 9-12, 1992.
2. O'Brien, T.K. "Toward a damage tolerance philosophy for composite materials and structures," Composite materials: Testing and Design, ASTM, STP 1059, 1990, pp.7-33.
3. Talreja, R. "Fatigue of composite materials," Published by Tech. publishing Co., 1987.
4. Tsai, S.W. "Composite Design- Fourth edition," Think Composites, 1988
5. Hwang, W. and Han, K.S. "Fatigue of composite materials-Damage model and life prediction," Composite Materials: Fatigue and Fracture, ASTM, STP 1012, 1989, pp. 87-102.
6. O'Brien, T.K. "Characterization of Delamination onset and growth in a composite laminate," Damage in Composite Materials , ASTP STP 775 1982, pp.140-167.
7. Broutman, I.J. and Sahu, S. "A new theory to predict cumulative fatigue damage in fibreglass reinforced plastics," Composite Materials: Testing and Design, ASTM STP 497, 1972, pp. 170-188.
8. Hahn, H. and Kim. R.Y. "Proof testing of composite materials," Journal of Composite Materials, Vol. 9, 1975, pp. 297-311.
9. Yang, J. N. and Liu, M.D. "Residual Strength degradation model and theory of periodic proof test for Graphite/epoxy laminates," Journal of Composite Materials, Vol. 11, 1977 PP. 176-203.
10. Charawize, A. and Daniel, I.M. "Damage mechanisms and accumulation in graphite/epoxy laminates," Composite Materials: Fatigue and Fracture, ASTM STP 907, 1986, PP. 274-297.
11. Reifsnider, K.L. and Stinchcomb, W.W. "A critical-elemental model of the

- residual strength and life of fatigue-loaded composite coupons," Composite Materials: Fatigue and Fracture, ASTM STP 907, 1986, pp.298-313.
12. Hahn, H.T. and Kim, R.Y. "Fatigue behavior of composite laminates," Journal of Composite Materials, Vol, 10, 1976, pp.150-180.
  13. O'Brien, T.K. and Reifsnider, K.L. "Fatigue damage evaluation through stiffness measurements in Boron-epoxy laminates," Journal of Composite Materials, Vol.15, 1981, pp. 55-70.
  14. O'Brien, T.K. "Analysis of local delamination and Their influence on composite laminate behavior," Delamination and Debonding of Materials, ASTM STP 876, 1985, PP. 282-297.
  15. Ganczakowski, H.L., Ashby, M.F., Beaumont, P.W.R. and Smith, P.A. "The behavior of Kevlar fibre-Epoxy laminates under static and fatigue loading-Part 2: Modelling," Composite Science and Technology 37(1990) pp. 371-392.
  16. Caslini, M., Zanotti, C. and O'Brien, T.K. "Study of matrix cracking and delamination in Glass/Epoxy laminates," Journal of Composites Technology and Research, Vol.9, No.4, 1987, PP.121-130.
  17. Beaumont, P.W.R. "The fatigue damage mechanics of composite laminates," ASTM STP 935 1985 pp. 53-62
  18. Lin, Y. "On fatigue damage accumulation and material degradation in composite materials," Composites Science and Technology 36(1989) pp.339-350.
  19. Highsmith, A.L. and Reifsnider, K.L. "Stiffness-Reduction Mechanisms in composite laminate," Damage in Composite materials, ASTM STP 775, 1982, pp 103-117.
  20. O'Brien, T.K., Rigamonti, M. and Zanotti, C. "Tension fatigue analysis and life prediction for composite laminates," International journal of Fatigue, 11, No. 6 1989 pp. 379-393.
  21. Jamison, R.D., Schulte, K., Reifsnider, K.L. and Stinchcomb, W.W. "Characterization and Analysis of Damage Mechanisms in tension-tension Fatigue of Graphite/epoxy laminates," ASTM STP 836 1984, PP.21-55.

22. Poursartip, A. and Chinatambi, N. "Fatigue damage development in notched  $[0_2/\pm 45]_s$  laminates," Composite Materials: fatigue and Fracture, ASTM STP 1012, 1989, pp. 45-65.
23. Ming-Hwa, R. J., Hsu, J. M. and Hwang, D.G. "Fatigue Degradation in centrally notched quasi-isotropic laminates," Journal of Composite Materials, Vol. 24, 1990, pp. 823-837.
24. Kress, G. R. and Stinchcomb, W. W. "Fatigue response of notched Graphite/Epoxy laminates," Recent Advances in Composites in the United States and Japan, ASTM STP 864, 1985, pp. 173-196.
25. Talreja, R. "Transverse cracking and stiffness reduction in cross ply laminates of different matrix toughness," The Danish Center for Applied Mathematics and Mechanics, the Technical University of Denmark, Report No. 428, June 1991.

## APPENDIX A

### RESIDUAL MODULI AND CRACK DENSITY

(from Talreja, R. [3])

Consider a two-dimensional solid containing  $m$  sets of parallel planar cracks. To each parallel planar crack, we assign a vector  $V$  oriented normal to the crack plane as illustrated in Figure A1 for two sets of parallel cracks. The vector  $V$  can be expressed by

$$V^{(i)} = D^{(i)} n^{(i)} \quad , \quad i=1,2,..m \quad (A1)$$

where  $D^{(i)}$  is the magnitude of the vector  $V^{(i)}$  and  $n^{(i)}$  is a unit vector oriented normal to the planes of the  $i$ th set of planar cracks.

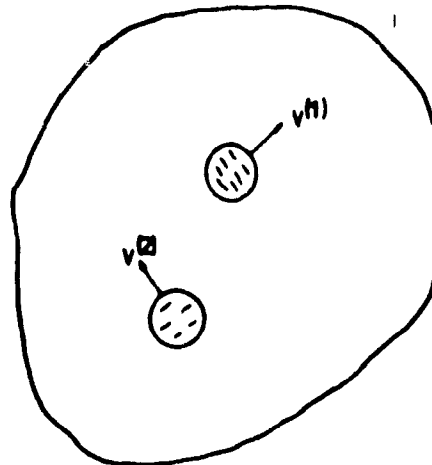


Fig. A1. A solid containing two sets of parallel cracks

For a set of same orientation cracks in a laminate, The vector magnitude is given

by,

$$D^2 = V \quad V = B_c l_c w_c \left(\frac{t_c}{t}\right) = \frac{K_m}{\sin\theta} \frac{t_c^2}{t} \quad (\text{A2})$$

where  $B_c$  is the number of cracks per unit surface area and  $l_c$  and  $w_c$  are the average length and width, respectively, of the cracks.  $t_c$  is the thickness of the plies containing the cracks and  $t$  is the total thickness of laminates.  $K_m$  and  $\theta$  is crack density and orientation angle of fiber, respectively.

Assuming that elastic strain energy function is a function of the strain tensor and damage vector sets  $V^{(i)}$ , and assuming further that the strain components and the damage vector magnitude are small, Talreja derive the elastic constitutive equations for a orthotropic laminate expressed as

$$\sigma_p = (C_{pq}^0 + \sum_{i=1}^m C_{pq}^i) \epsilon_q = C_{pq} \epsilon_q, \quad p, q = 1, 2, 6 \quad (\text{A3})$$

where

$$C_{pq}^0 = \begin{bmatrix} 2k_1 & k_2 & 0 \\ k_2 & 2k_6 & 0 \\ 0 & 0 & 2k_{10} \end{bmatrix} \quad (\text{A4})$$

and

$$C_{pq}^i = \begin{bmatrix} C_{11} & C_{12} & C_{16} \\ C_{21} & C_{22} & C_{26} \\ C_{61} & C_{62} & C_{66} \end{bmatrix} \quad (\text{A5})$$

where

$$\begin{aligned}
 C_{11} &= 2k_3 D_i^2 m_i^2 + 2k_4 D_i^2 n_i^2 \\
 C_{12} &= k_{13} D_i^2 m_i^2 + k_{14} D_i^2 n_i^2 \\
 C_{16} &= -0.5k_5 D_i^2 m_i n_i \\
 C_{22} &= 2k_7 D_i^2 m_i^2 + 2k_8 D_i^2 n_i^2 \\
 C_{26} &= -0.5k_9 D_i^2 m_i n_i \\
 C_{66} &= 2k_{11} D_i^2 m_i^2 + 2k_{12} D_i^2 n_i^2
 \end{aligned} \tag{A6}$$

where

$$m_i = \sin\theta_i, \quad n_i = \cos\theta_i; \quad C_{21} = C_{12}; \quad C_{61} = C_{16}; \quad C_{62} = C_{26}$$

$k_i$  in equation (A6) are material constants.  $C_{pq}^0$  is the stiffness matrix of the undamaged laminate which can be determined by laminate plate theory,  $C_{pq}^i$ ,  $i=1,2,\dots,m$ , are the stiffness reduction matrix components due to matrix cracking whose coefficients are functions of the component of the damage vector  $\mathbf{V}^{(i)}$ , and  $C_{pq}$  is the total stiffness matrix

For the case of one set of cracks, i.e.,  $m=1$ , Figure A2 shows a cross-ply laminate with cracks in the transverse plies and no cracks exist in the  $0^\circ$ -ply. The damage vector for this case is given by  $\mathbf{V}=D\{1,0\}$ , i.e.,  $\theta = 90$ . Substituting  $m=1$  and  $\theta = 90$  into equation (A6), and then into equation (A5), we obtain

$$C_{pq}^1 = \begin{bmatrix} 2k_3 D^2 & k_{13} D^2 & 0 \\ k_{13} D^2 & 2k_7 D^2 & 0 \\ 0 & 0 & 2k_{11} D^2 \end{bmatrix} \tag{A7}$$

The residual stiffness matrix due to matrix cracking becomes

$$C_{pq} = \begin{bmatrix} (2k_1+2k_3D^2) & (k_2+k_{13}D^2) & 0 \\ (k_2+k_{13}D^2) & (2k_6+2k_7D^2) & 0 \\ 0 & 0 & (2k_{10}+2k_{11}D^2) \end{bmatrix} \quad (A8)$$

The orthotropic symmetry in the coefficients of stiffness matrix is thus retained for this crack mode.

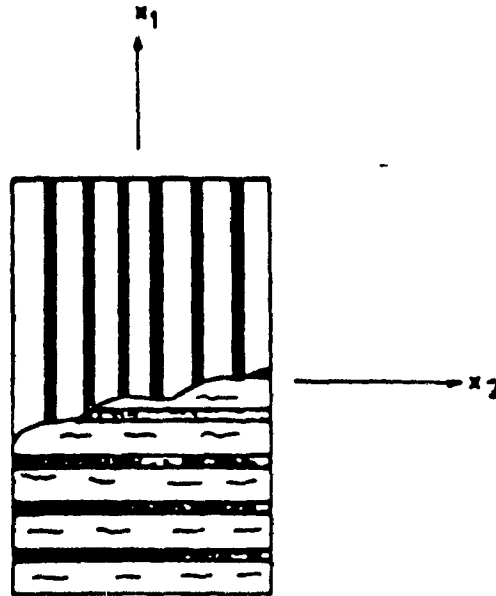


Fig. A2. A cross-ply laminate with cracks in the 90° ply

The residual elastic moduli can now be calculated by use of equation (A8)

$$\begin{aligned} E_1 &= E_1^0 + 2D^2[k_3 + k_7(v_{12}^0)^2 - k_{13}v_{12}^0] \\ E_2 &= E_2^0 + 2D^2[k_7 + k_3(v_{21}^0)^2 - k_{13}v_{21}^0] \\ v_{12} &= v_{12}^0 + D^2\left[\frac{1 - v_{12}^0v_{21}^0}{E_2^0}\right](k_{13} - 2k_7v_{12}^0) \\ G_{12} &= G_{12}^0 + 2D^2k_{11} \end{aligned} \quad (A9)$$

For the case of a laminate with two sets of cracks ( $m=2$ ), figure A3 shows two off-axis plies placed symmetrically about the axis  $X_1$ . The damage vectors in this case are

$$\begin{aligned} V_1 &= D_1 \{ \sin\theta, -\cos\theta \} \\ V_2 &= D_2 \{ \sin\theta, \cos\theta \} \end{aligned} \tag{A10}$$

Considering the case of  $\theta = 45^\circ$  and noting that  $k_3 = k_4$ ,  $k_7 = k_8$ , and  $k_{13} = k_{14}$  due to  $\sin\theta = \cos\theta$ , the residual stiffness matrix is obtained by use of equation (A3)

$$C_{pq} = C_{pq}^0 + C_{pq}^1 + C_{pq}^2 \tag{A11}$$

that is,

$$C_{pq} = \begin{bmatrix} [2k_1 + 2k_3(D_1^2 + D_2^2)] & [k_2 + k_{13}(D_1^2 + D_2^2)] & [\frac{1}{4}k_5(D_1^2 - D_2^2)] \\ & [2k_6 + 2k_7(D_1^2 + D_2^2)] & [\frac{1}{4}k_9(D_1^2 - D_2^2)] \\ \text{SYMMETRY} & & [2k_{10} + 2k_{11}(D_1^2 + D_2^2)] \end{bmatrix} \tag{A12}$$

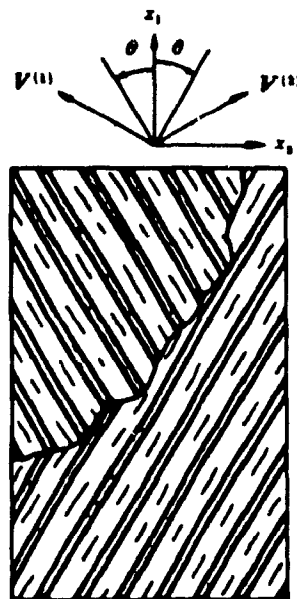


Fig. A3. Cracks in two plies symmetrically placed about the  $X_1$  axis

It is seen that, for  $D_1 = D_2$ , the orthotropic symmetry is retained. However, it is assumed that, even for  $D_1 \neq D_2$ , the orthotropic symmetry for the stiffness matrix will be retained approximately. It is reasonable assumption because the constants  $k_7$  and  $k_9$ , which represent the interactions between normal and shear strain, are often small. The residual elastic moduli for this case are given by

$$\begin{aligned}
 E_1 &= E_1^0 + 2(D_1^2 + D_2^2)[k_3 + k_7(v_{12}^0)^2 - k_{13}v_{12}^0] \\
 E_2 &= E_2^0 + 2(D_1^2 + D_2^2)[k_7 + k_3(v_{21}^0)^2 - k_{13}v_{21}^0] \\
 v_{12} &= v_{12}^0 + (D_1^2 + D_2^2) \left[ \frac{1 - v_{12}^0 v_{21}^0}{E_2^0} \right] (k_{13} - 2k_7 v_{12}^0) \\
 G_{12} &= G_{12}^0 + 2(D_1^2 + D_2^2)k_{11}
 \end{aligned} \tag{A13}$$

From the above analysis the laminates which contain  $0^\circ$ ,  $90^\circ$ , and  $\pm \theta$  plies if we neglect the coupling effects between normal and shear strain, the orthotropic symmetry will be maintained. The residual moduli for these cases can be given by

$$\begin{aligned}
 E_1 &= E_1^0 + 2D_m[k_3 + k_7(v_{12}^0)^2 - k_{13}v_{12}^0] \\
 E_2 &= E_2^0 + 2D_m[k_7 + k_3(v_{12}^0)^2 - k_{13}v_{21}^0] \\
 v_{12} &= v_{12}^0 + D_m \left[ \frac{1 - v_{12}^0 v_{21}^0}{E_2^0} \right] (k_{13} - 2k_7 v_{12}^0) \\
 G_{12} &= G_{12}^0 + 2D_m k_{11}
 \end{aligned} \tag{A14}$$

where

$$D_m = \sum_{i=1}^m D_i^2 \tag{A15}$$

The crack damage variable  $D_m$ , for example, can be expressed for the  $[0/90/\pm\theta]_s$

laminate by

$$D_m = (D_{90}^2 + D_0^2 + D_{-0}^2) \quad (\text{A16})$$

The material constants  $k_3$ ,  $k_7$  and  $k_{13}$  were given for the glass/epoxy laminate to be

$$k_3 = -6.713 \text{ GPa} , k_7 = -0.762 \text{ GPa} , k_{13} = -4.467 \text{ GPa}$$

and for the graphite/epoxy laminate

$$k_3 = -17.875 \text{ GPa} , k_7 = -0.141 \text{ GPa} , k_{13} = -5.557 \text{ GPa}$$

Due to the uncertainty in measurement of the shear modulus Ramesh Talreja does not give the constant  $k_{11}$ . However, this does not affect determination of the remaining constants. We assume in this research that shear modulus may have same reduction ratio as that of longitudinal modulus approximately due to lack of experimental data, i.e.,

$$\frac{E_2}{E_2^0} = \frac{G_{12}}{G_{12}^0} \quad (\text{A17})$$

It is easy to obtain

$$\frac{k_{11}}{G_{12}^0} = \frac{[k_7 + k_3(v_{21}^0)^2 - k_{13}v_{21}^0]}{E_1^0} \quad (\text{A18})$$

From above equations developed by Talreja [3] and slightly extended by this research, we can see that the relations between residual elastic moduli and matrix cracking damage have been established. The proposed equations have good agreement with experimental data [3].

## APPENDIX B

### ONSET OF LOCAL DELAMINATION

(from O'Brien, T.K. [2,14])

#### B.1 STRAIN ENERGY RELEASE RATE

For an elastic body containing a crack that grows under a constant applied load,  $P$ , the strain energy release rate,  $G$ , is given by

$$G = \frac{P^2 dC}{2 dA} \quad (\text{B1})$$

where  $C$  is the compliance and  $A$  is the crack surface area created. A similar expression may be written for  $G$  in terms of the remote stress,  $\sigma$ , and the compliance of elastic body,  $S$ , by substituting

$$C = \frac{Sl}{wt} \quad (\text{B2})$$

into equation (B1). This yields

$$G = \frac{1}{2} V \sigma^2 \frac{dS}{dA} \quad (\text{B3})$$

where  $dS/dA$  is the rate of changes in  $S$  as the flow extends, and  $V$  is the volume of the body. For the case where the elastic body is a composite laminate containing a matrix ply crack through the thickness of  $n$  off-axis plies, with delamination forming at the matrix crack tip and growth in the ply interfaces (Fig.B1), the strain energy release rate associated with the growth of delamination from a single matrix crack will be considered.

considered. In order to evaluate  $dS/dA$  in equation (B3), an equation for laminate compliance as a function of delamination size was developed.

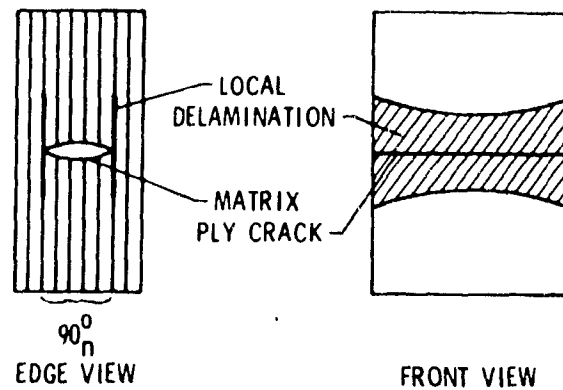


**Fig. B1** Depiction of local delamination growing from matrix cracks

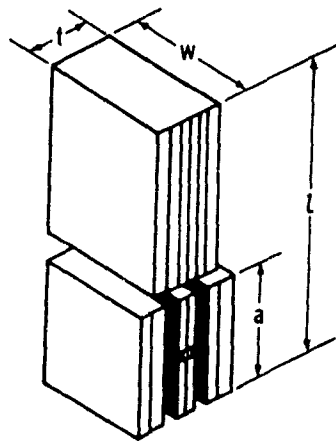


**Fig. B2** Model of local delamination

Figure B2 illustrates a composite laminate containing delaminations growing from a matrix ply crack. The composite gage length,  $l$ , is divided into a locally delaminated region,  $a$ , and a laminated region  $l-a$ . Assuming the composite displacements are the sum of the displacements in these two regions, and the total load,  $P$ , is equal to the loads carried by the two regions individually, then using Hooke's law,  $\Delta l = Pl/AE$ , yields

$$S = \frac{1}{E} = \frac{A_{lam}}{l} \left[ \frac{(l-a)}{A_{lam}E_{lam}} + \frac{a}{A_{ld}E_{ld}} \right] \quad (B4)$$

where  $A_{lam}$  and  $E_{lam}$  are the cross-sectional area and modulus of the laminated region, and  $A_{ld}$  and  $E_{ld}$  are the cross-sectional area and modulus of the locally delaminated region. Each of the areas in equation (B4) represents only the cross-sectional area that carries the applied load; hence

$$A_{lam} = w t \quad (B5)$$

$$A_{ld} = w t_{ld} \quad (B6)$$

where  $w$  and  $t$  are the laminate width and thickness, respectively, and  $t_{ld}$  is the thickness of the locally delaminated region that carries load (i.e., the thickness of the uncracked plies). Substituting equations (B5) and (B6) into equation (B4) yields

$$S = \frac{a t}{l} \left( \frac{1}{t_{ld}E_{ld}} - \frac{1}{tE_{lam}} \right) + \frac{1}{E_{lam}} \quad (B7)$$

Returning to figure (B2) the strain energy release rate associated with the growth of delamination from a matrix ply crack can be calculated by assuming

$$\begin{aligned} V &= twl \\ A &= nwa \\ dA &= nwda \end{aligned} \quad (B8)$$

where  $n$  is the number of delamination growing from the matrix ply crack. For the case illustrated in figure (B2),  $n=2$ , but for a delamination growing from a cracked surface ply,  $n=1$ . Substituting equation (B8) into equation (B3) and differentiating equation (B7) yields

$$G = \frac{\sigma^2 t^2}{2n} \left( \frac{1}{t_{ld}E_{ld}} - \frac{1}{tE_{lam}} \right) \quad (B9)$$

Hence, as indicated in equation (B9), the strain energy release rate is independent of delamination size. The magnitude of  $G$  depends only on the laminate layup and thickness, the location of the cracked ply and subsequent delamination (which determines  $E_{ld}$ ,  $t_{ld}$ , and  $n$ ), the applied load,  $P$ , and the laminate width,  $w$ .

## B.2 PREDICTION OF LOCAL DELAMINATION ONSET

In order to predict the onset of local delamination with fatigue cycles, the  $G$  versus  $\log N$  characterization of the composite material must be generated. Data from several materials with brittle and tough matrices indicate that between  $10^0 \leq N \leq 10^6$  cycles, the maximum cyclic  $G$  may be represented as a linear function of  $\log N$  (figures B3 and B4), where  $N$  is the number of cycles to delamination onset at a prescribed  $G_{max}$ . Hence,

$$G = m \log N + G_c \quad (B10)$$

where  $G_c$  and  $m$  are material parameters that characterize the onset of delamination under static and cyclic loading in the material. This characterization may be accomplished using a variety of interlaminar fracture test methods. Next,  $G$  must be calculated for the first local delamination that will form. This typically occurs at a matrix crack in the surface ply but it may be confirmed by calculating  $G$  for matrix cracking in all of the off-axis plies in the laminate. The one with the highest  $G$  for the same applied load will be the first to form. This  $G$  may be calculated using equation (B9). In order to calculate the number of cycles for the first local delamination to form,  $N_1$ , equation (B9) is set equal to equation (B10) and then solved for  $N_1$ . Hence,

$$\log N_1 = \frac{1}{m} \left[ \frac{\sigma^2 t^2}{2n} \left( \frac{1}{t_{ld} E_{ld}} - \frac{1}{t E_{lam}} \right) - G_c \right] \quad (B11)$$

Equation (B11) can be used for predicting the onset of local delamination under cyclic loading.

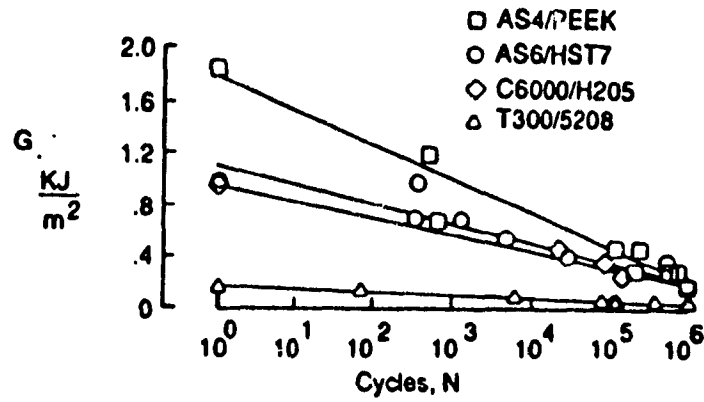


Fig. B3 Strain energy release rate at delamination onset as function of fatigue cycles

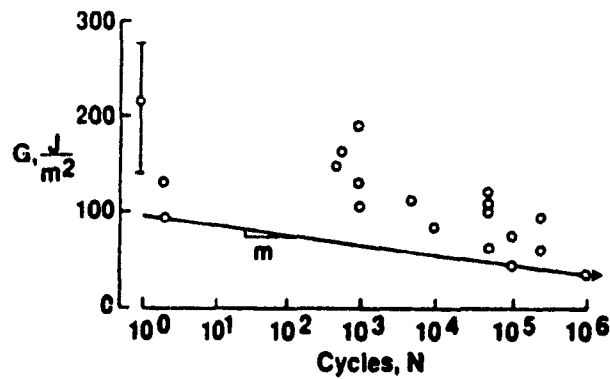


Fig. B4 Strain energy release rate at delamination onset as function of fatigue cycles for X751/50 E-glass/epoxy

## APPENDIX C

### COMPUTER CODES

#### COMPUTER CODE 1.

---

THIS PROGRAM IS TO GENERATE A NASTRAN PROGRAM  
CODE FOR STRESS ANALYSIS AND PLOTTING  
( GENNAS )

---

C  
C GENERATING A GRID PLOT FOR FEM  
C

```
CLEAR , , 2000
DIM x(250), y(250), A(100)
CLS
B = 26
w = 19
R = 9.5 / 2
m = 33
A = 3.14159 / (2 * (m - 1))
NUM = 0
FOR i = 1 TO m
  K = i - 1
  x(i) = R * COS(A * K)
  y(i) = R * SIN(A * K)
  A(i) = A * K * 180 / 3.14159
  x(m + i) = 1.2 * R * COS(A * K)
  y(m + i) = 1.2 * R * SIN(A * K)
NEXT
FOR i = 1 TO ((m + 1) / 2)
```

```
K = j - 1
x(2 * m + i) = 1.5 * R * COS(2 * A * K)
y(2 * m + i) = 1.5 * R * SIN(2 * A * K)
x((5 * m + 1) / 2 + i) = 2 * R * COS(2 * A * K)
y((5 * m + 1) / 2 + i) = 2 * R * SIN(2 * A * K)
NUM = (5 * m + 1) / 2 + i
NEXT
FOR i = 1 TO ((m + 1) / 4 + 1)
K = i - 1
x(NUM + i) = 2.5 * R * COS(4 * A * K)
y(NUM + i) = 2.5 * R * SIN(4 * A * K)
NUM1 = NUM + i
NEXT
FOR i = 1 TO ((m + 1) / 4 + 1)
K = i - 1
x(NUM1 + i) = 3 * R * COS(4 * A * K)
y(NUM1 + i) = 3 * R * SIN(4 * A * K)
NUM2 = NUM1 + i
NEXT
FOR i = 1 TO ((m + 1) / 4 + 1)
K = i - 1
x(NUM2 + i) = 3.5 * R * COS(4 * A * K)
y(NUM2 + i) = 3.5 * R * SIN(4 * A * K)
NUM3 = NUM2 + i
NEXT
FOR j = 1 TO 6
n = j - 1
x(NUM3 + j) = 4 * R
y(NUM3 + j) = w * n / 5
NUM4 = NUM3 + j
NEXT
mmm = ((m + 1) / 2 + 1) / 2
FOR l = 1 TO mmm - 5
x(NUM4 + l) = 4 * R - (4 * R / (mmm - 6)) * l
y(NUM4 + l) = w
NUM5 = NUM4 + l
NEXT
FOR j = 1 TO 6
n = j - 1
x(NUM5 + j) = 4 * R + B / 2
y(NUM5 + j) = w * n / 5
NUM6 = NUM5 + j
NEXT
```

```

FOR j = 1 TO 6
n = j - 1
x(NUM6 + j) = 4 * R + B
y(NUM6 + j) = w * n / 5
NUM7 = NUM6 + j
NEXT
FOR i = 1 TO 100
PRINT "I, X, Y, A(i)= "; i, x(i), y(i), A(i)
NEXT

```

C

C GENERATING GRAPHICS FOR PLOTTER (SEE Fig.7.3)

C

```

SCREEN 12
COLOR 10
CLS
VIEW (104, 5)-(536, 430), , 1
WINDOW (0, 0)-(4 * R + B, 4 * R + B)
CLS 0
LINE (0, 0)-(4 * R, w), , B
LINE (0, 0)-(4 * R + B, w), , B
FOR i = 2 TO m
LINE (x(i), y(i))-(x(i - 1), y(i - 1))
NEXT
FOR j = m + 2 TO 2 * m
LINE (x(j), y(j))-(x(j - 1), y(j - 1))
LINE (x(j), y(j))-(x(j - m), y(j - m))
NEXT
mm = (m + 1) / 2
FOR kk = 1 TO mm - 1
jj = 2 * kk - 1
LINE (x(jj + m), y(jj + m))-(x(kk + 2 * m), y(kk + 2 * m))
LINE (x(2 * kk + m), y(2 * kk + m))-(x(kk + 2 * m), y(kk + 2 * m))
LINE (x(2 * kk + m), y(2 * kk + m))-(x(kk + 1 + 2 * m), y(kk + 1 + 2 * m))
NEXT
FOR K = 2 * m + 2 TO 2 * m + mm
LINE (x(K), y(K))-(x(K - 1), y(K - 1))
NEXT
FOR j = 2 * m + mm + 2 TO NUM
LINE (x(j), y(j))-(x(j - 1), y(j - 1))
LINE (x(j), y(j))-(x(j - mm), y(j - mm))

```

```

NEXT
nm = 2 * m + mm
mmm = (mm + 1) / 2
FOR kk = 1 TO mmm - 1
jj = 2 * kk - 1
LINE (x(jj + nm), y(jj + nm))-(x(kk + NUM), y(kk + NUM))
LINE (x(2 * kk + nm), y(2 * kk + nm))-(x(kk + NUM), y(kk + NUM))
LINE (x(2 * kk + nm), y(2 * kk + nm))-(x(kk + 1 + NUM), y(kk + 1 + NUM))
NEXT
FOR i = NUM + 2 TO NUM1
LINE (x(i), y(i))-(x(i - 1), y(i - 1))
NEXT
FOR j = NUM1 + 2 TO NUM2
LINE (x(j), y(j))-(x(j - 1), y(j - 1))
LINE (x(j), y(j))-(x(j - mmm), y(j - mmm))
NEXT
FOR K = NUM2 + 2 TO NUM3
LINE (x(K), y(K))-(x(K - 1), y(K - 1))
LINE (x(K), y(K))-(x(K - mmm), y(K - mmm))
NEXT
FOR i = NUM3 + 2 TO NUM5
LINE (x(i), y(i))-(x(i - 1), y(i - 1))
NEXT
FOR j = 1 TO 6
LINE (x(NUM3 + j), y(NUM3 + j))-(x(NUM2 + j), y(NUM2 + j))
NEXT
FOR j = 7 TO (NUM5 - NUM3)
LINE (x(NUM3 + j), y(NUM3 + j))-(x(NUM2 + j), y(NUM2 + j))
NEXT
FOR i = 1 TO 6
LINE (x(NUM3 + i), y(NUM3 + i))-(x(NUM5 + i), y(NUM5 + i))
LINE (x(NUM5 + i), y(NUM5 + i))-(x(NUM6 + i), y(NUM6 + i))
NEXT
FOR i = 2 TO 6
LINE (x(NUM5 + i), y(NUM5 + i))-(x(NUM5 + i - 1), y(NUM5 + i - 1))
NEXT

```

C

C **GENERATING PROGRAM CODE FOR NASTRAN SOFTWARE**

C

```

OPEN "FEMC.DAT" FOR OUTPUT AS #1
FOR i = 1 TO NUM7

```

```

PRINT #1, "GRAD,"; i, ", ", x(i); ", ", y(i); ", ", "0"
NEXT
FOR i = 1 TO m - 1
PRINT #1, "CQUAD4,"; i, ", ", "10,"; i, ", ", m + i, ", ", m + 1 + i, ", ", i + 1, ", ", -A(i)
NEXT
K = 0
j = m
FOR i = m + 2 TO 2 * m - 1 STEP 2
K = K + 1
j = j + 3
ANG = -(180 / 3.141159) * ATN((y(2 * m + K) - y(i - 1)) / (x(2 * m + K) - x(i - 1)))
PRINT #1, "CTRIA3,"; j - 3, ", ", "10,"; i - 1, ", ", 2 * m + K, ", ", i, ", ", ANG
ANG = -(180 / 3.141159) * ATN((y(2 * m + K) - y(i)) / (x(2 * m + K) - x(i)))
PRINT #1, "CTRIA3,"; j - 2, ", ", "10,"; i, ", ", 2 * m + K, ", ", 2 * m + 1 + K, ", ", ANG
ANG = -(180 / 3.141159) * ATN((y(2 * m + K + 1) - y(i)) / (x(2 * m + K + 1) - x(i)))
PRINT #1, "CTRIA3,"; j - 1, ", ", "10,"; i, ", ", 2 * m + K + 1, ", ", i + 1, ", ", ANG
jj = j - 1
NEXT
mmm = 2 * m + mm
FOR i = 2 * m + 1 TO mmm - 1
jj = jj + 1
PRINT #1, 'CQUAD4,"; jj; ", ", "10,"; i, ", ", mm + i, ", ", mm + 1 + i, ", ", i + 1
NEXT
K = 0
j = jj + 1
FOR i = 2 * m + mm + 2 TO NUM STEP 2
K = K + 1
j = j + 3
PRINT #1, "CTRIA3,"; j - 3, ", ", "10,"; i - 1, ", ", NUM + K, ", ", i
PRINT #1, "CTRIA3,"; j - 2, ", ", "10,"; i, ", ", NUM + K, ", ", NUM + K + 1
PRINT #1, "CTRIA3,"; j - 1, ", ", "10,"; i, ", ", NUM + K + 1, ", ", i + 1
jj = j - 1
NEXT
mmm = (mm + 1) / 2
FOR i = NUM + 1 TO NUM1 - 1
jj = jj + 1
PRINT #1, "CQUAD4,"; jj; ", ", "10,"; i, ", ", i + mmm, ", ", mmm + 1 + i, ", ", i + 1
NEXT
FOR i = NUM1 + 1 TO NUM2 - 1
jj = jj + 1
PRINT #1, "CQUAD4,"; jj; ", ", "10,"; i, ", ", i + mmm, ", ", mmm + 1 + i, ", ", i + 1
NEXT
FOR i = NUM2 + 1 TO NUM3 - 1

```

```
jj = jj + 1
PRINT #1, "CQUAD4,"; jj; ", "; "10,"; i; ", "; i + mmm; ", "; mmm + 1 + i; ", "; 1 + i
NEXT
FOR i = NUM3 + 1 TO NUM4 - 1
jj = jj + 1
PRINT #1, "CQUAD4,"; jj; ", "; "10,"; i; ", "; i + mmm; ", "; mmm + 1 + i; ", "; 1 + i
NEXT
FOR i = NUM5 + 1 TO NUM6 - 1
jj = jj + 1
PRINT #1, "CQUAD4,"; jj; ", "; "10,"; i; ", "; i + 6; ", "; 7 + i; ", "; 1 + i
NEXT
PRINT #1, "MUN, -NUM7"; NUM; NUM1; NUM2; NUM3; NUM4; NUM5; NUM6; NUM7
CLOSE #1
END
```

**COMPUTER CODE 2.**

---

THIS PROGRAM IS DEVELOPED IN NASTRAN LANGUAGE FOR STRESS  
ANALYSIS AND PREDICTION OF FAILURE MECHANISMS OF NOTCHED  
COMPOSITE LAMINATES UNDER CYCLIC LOADING  
( NASCOM )

---

\$  
\$ NASTRAN EXECUTIVE CONTROL DECK  
\$

/INF MVS CL(90) ROUTE (MUSICA) TI(40)  
// EXEC MASTRAN  
SOL 24  
DIAG 49,44  
TIME 40  
.. BM 2 RF24D79  
CEND

\$  
\$ CASE CONTROL DECK  
\$

TITLE= ANALYSIS OF FEM FOR COMPOSITE  
SUBTITLE= MATERIAL PROPERTIES OF PLATE ELEMENT  
SUBCASE=1  
ECHO = BOTH  
LOAD = 1  
OUTPUT  
DISP = ALL  
FORCE = ALL

STRESS = ALL  
STRAIN = ALL  
GPFORCE = ALL  
OLOAD = ALL  
GPSTRESS = ALL  
BEGIN BULK

\$

\$ INPUT BULK DATA DECK

\$

\$ INPUT DATA FILE "FEMC.DAT"

PARAM, AUTOSPC, YES

PCOMP, 10, -0.5, ,1000.0 ,HOFF

, 100, 1.0, 0.0, YES

MAT8, 100, 69.68+9, 69.68+9, 0.3 , 26.88+9

ENDDATA

**COMPUTER CODE 3.**


---

THIS PROGRAM IS DEVELOPED FOR COMPUTING  
RESIDUAL ELASTIC MODULI OF A NOTCHED COMPOSITE LAMINATE  
UNDER CYCLIC LOADING (EQ. (81) TO EQ.(83))  
( RMODULI )

---

```

INPUT "N=?, SIGMA1=?,SIGMA2=?", N,SIGMA1,SIGMA2
E10 = 69.68
E20 = E10
Es0 = 26.88
v120 = .3
K3 = -17.875
K7 = -.141
K13 = -5.557
KK = 1.16 * (10) ^ (-50 / 17.3)
b = 17.3
BB = 6
q = .8
Cm = -2 * (K3 + K7 * (v120) ^ 2 - K13 * v120) / E10
Dm = ((KK * N ^ (1 / b) * sigma1) ^ (b / BB)) * (1 - q) / Cm
E1 = E10 + 2 * Dm * (K3 + K7 * (v120) ^ 2 - K13 * v120)
E2 = E20 + 2 * Dm * (K7 + K3 * (v120) ^ 2 - K13 * v120)
v12 = v120 + Dm * (1 - v120 * v120) * (K13 - 2 * K7 * v120) / E20
Es = Es0 * E2 / E20
PRINT Dm; Cm; E1; E2; Es; v12
BB = 8
DDm = ((KK * N ^ (1 / b) * sigma2) ^ (b / BB)) * (1 - q) / Cm
EE1 = E10 + 2 * DDm * (K3 + K7 * (v120) ^ 2 - K13 * v120)
EE2 = E20 + 2 * DDm * (K7 + K3 * (v120) ^ 2 - K13 * v120)
vv12 = v120 + DDm * (1 - v120 * v120) * (K13 - 2 * K7 * v120) / E20
EEs = Es0 * EE2 / E20
EEE1 = E1 - (E20 - EE2)
EEE2 = E2 - (E10 - EE1)

```

```
nu12 = v12 - (v120 - vv12)
EEEs = Es - (Es0 - EEs)
PRINT "E1,E2,Es, v12="; EEE1; EEE2; EEEs; nu12
END
```